

# Burdigalian-Serravallian (Miocene) radiolarians from Havelock Island, Northeast Indian Ocean and their paleoecological significance

Rikee Dey<sup>1,2</sup>, Amit K. Ghosh<sup>1\*</sup>, Lopamudra Roy<sup>1</sup>, Arindam Chakraborty<sup>1</sup>,  
Ajoy Kumar Bhaumik<sup>2</sup> and Stuti Saxena<sup>1</sup>

<sup>1</sup>*Birbal Sahni Institute of Palaeosciences, 53 University Road, Lucknow - 226 007, Uttar Pradesh, India*

<sup>2</sup>*Department of Applied Geology, Indian Institute of Technology (Indian School of Mines), Dhanbad - 826 004, Jharkhand, India*

\*Corresponding author email: akgosh\_in@yahoo.com, amitbsip@gmail.com

**ABSTRACT:** A detailed study on radiolarian biostratigraphy and paleoecology has been carried out from three outcrops on Havelock Island, belonging to the Ritchie's Archipelago of Andaman and Nicobar Group of islands. Though most of the radiolarian taxa are moderately preserved, it was possible to demarcate an age ranging from late early to early middle Miocene based on index radiolarians of RN4 and RN5 zones. An attempt has been made to correlate the radiolarian events recorded herein with earlier reports on radiolarians from different DSDP, ODP, and IODP sites of the Indian Ocean and the onshore sections of different islands of the Andaman and Nicobar Basin. A total of 119 radiolarian taxa belonging to 70 genera have been recorded in the present study, out of which 4 species are being reported for the first time from the northeastern part of the Indian Ocean. Diversity analyses were performed to deduce the Shannon Diversity Index, Simpson Index, Margalef Richness, and Pielou's Evenness. The Water Depth Ecology index (WADE) has been analyzed for a better understanding of the paleoecological perspectives, and the Nassellaria-Spumellaria ratio of each outcrop has been calculated to ascertain the water depth. Comparison of the data obtained from diversity analysis and WADE index provides a clear picture of the environment during the late early to early middle Miocene. The overwhelming dominance of warm species of radiolarians may be linked to the Miocene Climate Optimum (MCO) event.

**Key words:** Radiolaria, Biostratigraphy, Late early to early middle Miocene, Water Depth Ecology, Andaman-Nicobar Basin.

## INTRODUCTION

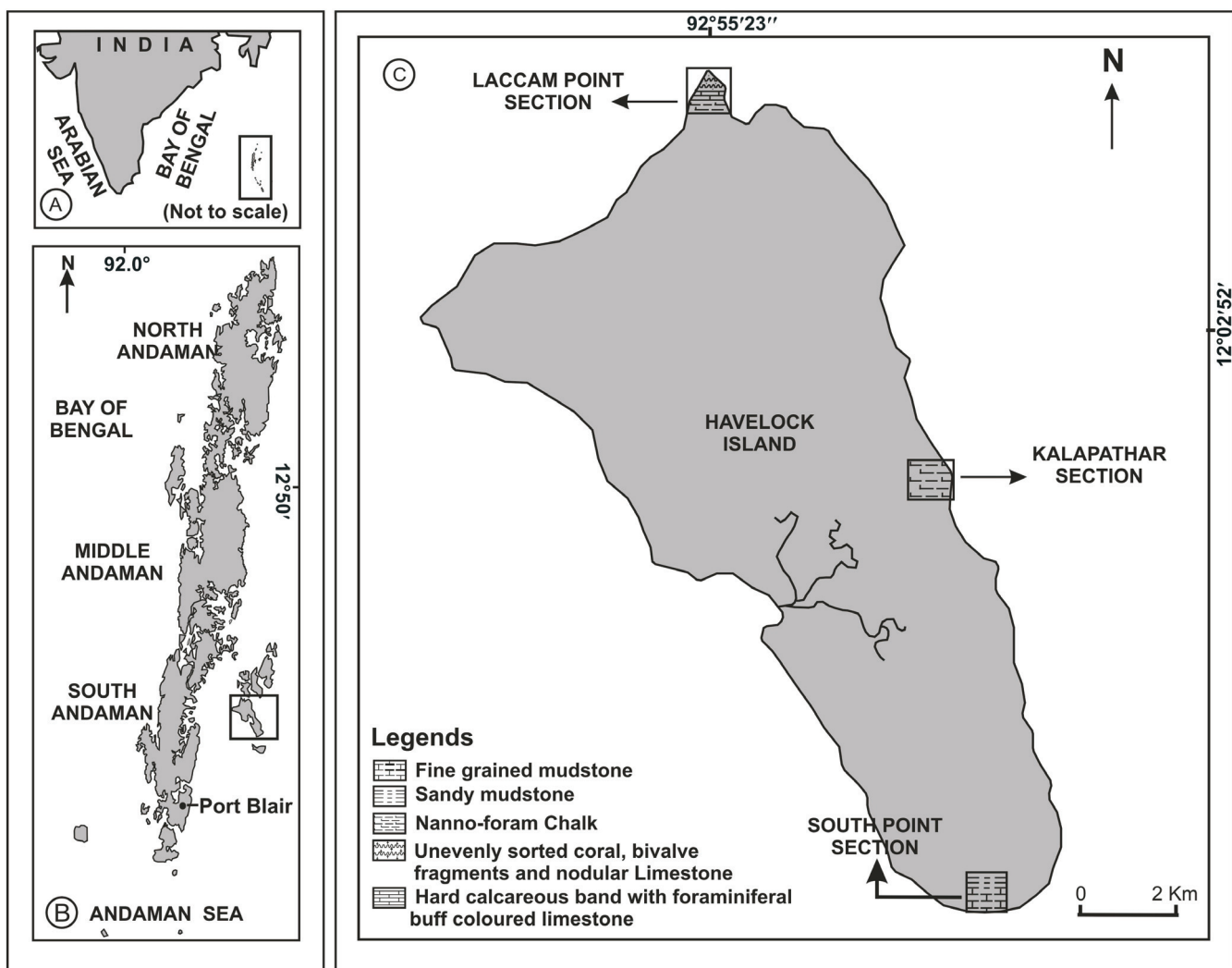
Radiolarians, the siliceous polycystina, are one of the excellent marine microfossils which provide considerable information regarding the past environment. Radiolarians are immensely helpful to decipher the stratigraphic age, depth, paleoclimate, and paleotemperature (Armstrong and Brasier 2005). Zoogeographies of radiolarians are interrelated with ocean circulation and water mass distribution (Armstrong and Brasier 2005). They are also useful indicators of paleogeographic and tectonic changes in ocean basins (Casey et al. 1990). The Andaman and Nicobar Group of islands is one of the most ideal places in this part of the world, where marine sediments are well exposed on different islands that ranges from late Mesozoic to Quaternary (Rajshekhar and Reddy 2003; Bandopadhyay and Carter 2017). Almost a complete sequence of Neogene marine sediments is exposed in the Andaman-Nicobar Basin (Sharma and Srinivasan 2007). These Neogene sediments archive well-preserved foraminifers (both benthic and planktonic), radiolarians, calcareous nannofossils, diatoms, and various other microfossils (Sharma and Srinivasan 2007 and references therein). Neogene sediments, specifically the Miocene sequence, are well exposed in three isolated outcrops that are accessible on Havelock Island.

There are some previous contributions on diatoms, radiolarians, and calcareous nannofossils from Havelock Island. Pant and Bandopadhyay (1972) reported calcareous nannofossils and Mathur (1973) reported some diatom taxa from the early Mi-

cene sequence of Havelock Island. Sharma and Ram (2003) reported a radiolarian assemblage from a single outcrop situated on the south coast of Havelock Island. A late early to early middle Miocene calcareous nannofossil assemblage was recorded by Singh (2007), and Chakraborty et al. (2019) studied the diatoms and correlated the diatom assemblages with calcareous nannofossils and radiolarians from this island. Recently, Saxena et al. (2021) published a comprehensive account on the diatoms, and Chakraborty et al. (2021) analyzed in detail the calcareous nannofossils from Havelock Island.

Radiolarian assemblages were reported earlier from the Miocene onshore sections of isolated islands of Andaman-Nicobar Basin such as Colebrook, North Passage and Great Nicobar islands (Mahapatra and Sharma 1994; Sharma and Ram 2003; Sharma et al. 2011), Nicholson Island (Sharma and Daneshian 1998; 2003; Sharma and Ram 2003), John Lawrence Island (Sharma and Daneshian 1998), Strait, Havelock and Henry Lawrence islands (Sharma and Ram 2003), Inglis Island (Sharma et al. 2007), Nancowry and Kamorta islands (Sharma et al. 1999; Sharma and Daneshian 2003).

It is well known that in the Miocene Epoch various floral and faunal evolutions took place. Within this epoch, there is evidence of global warming which is popularly known as the Miocene Climate Optimum i.e., MCO (Flower and Kennett 1994; Ramsay et al. 1998; Blois and Hadly 2009; McInerney and Wing 2011; Figueirido et al. 2012; Holbourn et al. 2015; Chakraborty et al. 2019; Modestou et al. 2020 and references



TEXT-FIGURE 1

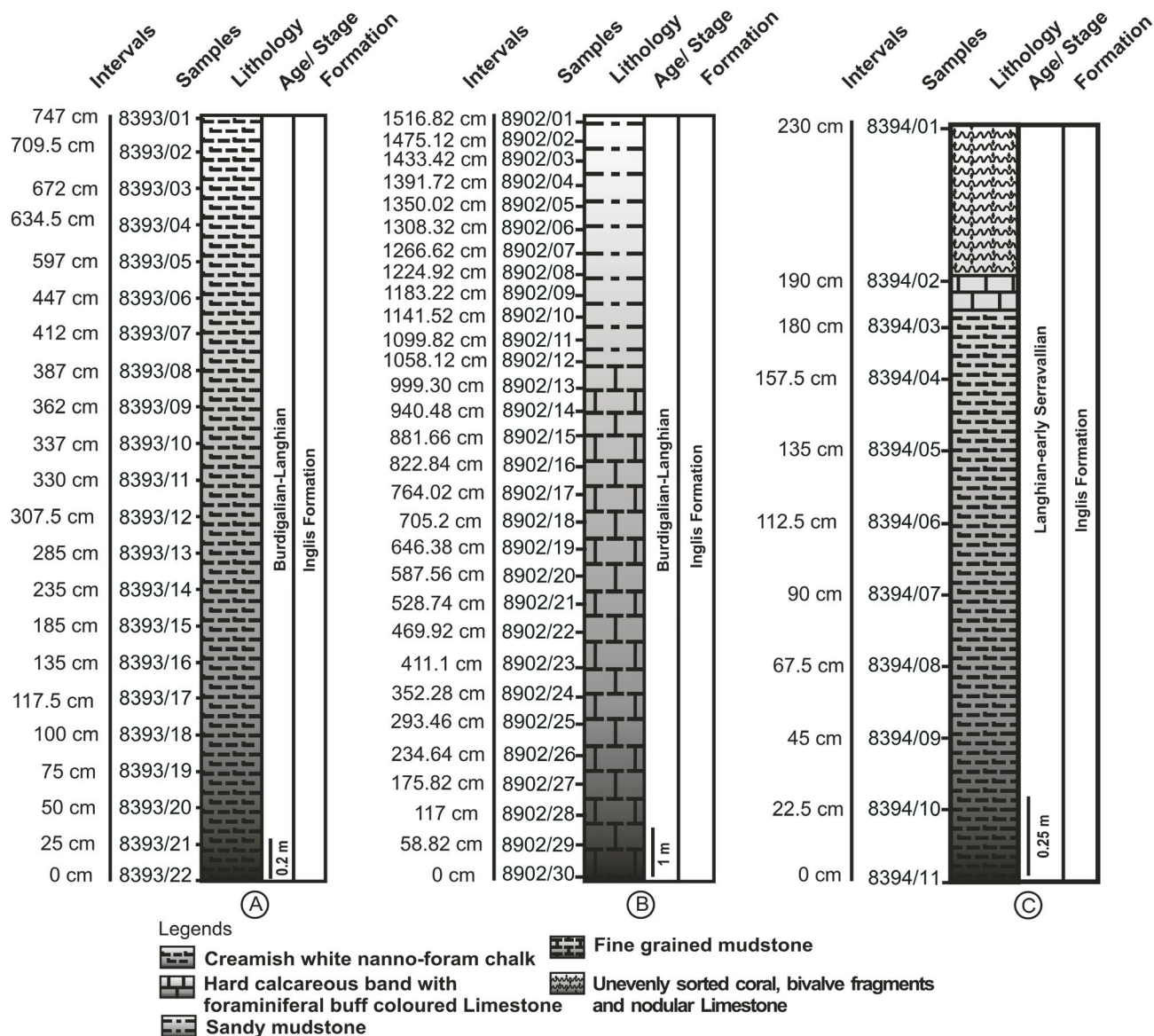
A. Map showing the Andaman and Nicobar Islands in the northeastern part of the Indian Ocean marked by a rectangle, B. Map showing the Havelock Island (marked by a rectangle) of Ritchie's Archipelago, C. Geological map of Havelock Island showing the sampling sites (modified after Sharma and Srinivasan 2007).

therein). Previous studies on radiolarians from the onshore sections of Andaman and Nicobar Basin were focused on biostratigraphy, however, the present study on radiolarians has been undertaken on Havelock Island which is focused on the diversity as well as biostratigraphy of radiolarians and to interpret the paleoecology based on WADE analysis. In addition, for determining the water depth Nassellaria-Spumellaria ratio was taken into consideration.

#### GEOLOGICAL SETTINGS

The Andaman-Nicobar subduction zone is tectonically very active and it is situated between 6°N and 14°N in the northeastern part of the Indian Ocean (text-fig. 1A), which is considered as one of the most seismically active regions on the earth (Singh and Moeremans 2017). Here the subduction of the Indian Plate beneath the Eurasian Plate took place and this collision has a major role in the tectonic evolution of this part of the world. The Andaman-Nicobar Basin has been regarded as a complex

active back-arc extensional basin that delineates the western boundary of the Andaman Sea. This forearc basin is composed of 3-3.5 km thick Cenozoic sediments that archive the evolution of the basin over the past ~60 Ma. Within this basin, there are two distinct deposits: Andaman Flysch Group and the Archipelago Group. The Andaman Flysch Group is about 3 km thick and belongs to late Eocene to Oligocene. The Andaman Flysch Group is unconformably overlain by the Archipelago Group of Neogene sediments which were deposited in an outer shelf to open-marine setting (Chakraborty and Pal 2001). During the Neogene period, some significant events took place i.e., a complete extinction of the Tethys Sea, Himalayan uplift, development of the Bengal Fan, and an appearance of the Andaman Sea (Srinivasan 1986; Sharma and Srinivasan 2007). During the Neogene, the continents attained their present position and shape. The faunal and floral turnover was accompanied by changes in both surface and deep-water ocean circulation during the Neogene (Sharma and Srinivasan 2007). Amongst the Andaman and Nicobar Group of islands, Ritchie's Archipelago



TEXT-FIGURE 2  
Lithologs of the outcrops: A. Kalapathar Section B. South Point Section C. Laccam Point Section.

Group is the top-most stratigraphic unit of the Neogene sequence ranging from early Miocene to Pleistocene. Srinivasan (1978) proposed nine regional stages and two regional series for the Neogene based on planktonic foraminiferal events. The lowermost series is divided into six regional stages belonging to Miocene. They are the Andamanian, Jawarian, Inglianian, Ongeian, Havelockian, and Neillian regional stages (Sharma and Srinivasan 2007).

Havelock Island is around 41 km northeast of the capital city, Port Blair (text-fig. 1B) and it is the largest island of Ritchie's Archipelago. On Havelock Island, there are two lithological units: the Ingli and Long formations which are exposed along the cliffs adjacent to the seashore. Lithologically, it is defined by nanno-foram chalk and calcareous mudstones. These sediments contain moderately preserved siliceous microfossils and

calcareous nannofossils. Based on planktonic foraminiferal zones (*Catapsydrax stainforthi* and *Neogloboquadrina acostensis*), Srinivasan and Azmi (1976) assigned an early to late Miocene age for the two lithological formations that chronostratigraphically belongs to the Havelockian Regional Stage correlateable to the Burdigalian to Serravallian international stage.

#### MATERIALS AND METHODS

For the present study samples were collected from three different outcrops: Kalapathar, South Point, and Laccam Point sections on Havelock Island (text-fig. 1C). From the outcrop of Kalapathar (12°00.20' N, 93°00.40' E) twenty two samples were collected (text-fig. 2A). The thickness of the outcrop is 7.47 m, and it is lithologically characterized by soft, creamish,

nanno-foram chalk with interbedded calcareous silty bands. Thirty samples were collected from the South Point Section ( $11^{\circ}53'113''$  N,  $93^{\circ}01.892'$  E) which is ~15 m in thickness (text-fig. 2B). Lithologically, it consists of fine-grained mudstone and sandy mudstone. The Laccam Point Section ( $12^{\circ}02'93''$  N,  $92^{\circ}57.91'$  E) is only 2.3 m thick, the rest of the cliff section is inaccessible due to thick vegetation cover. The sediments of the Laccam Point outcrop are composed of nanno-foram chalk at the base along with a hard, calcareous band of buff coloured foraminiferal limestone on the top, which is overlain by unevenly sorted nodular limestone with coral rags and bivalve fragments. Eleven samples were collected from this outcrop (text-fig. 2C).

For the study of the radiolarians, 2 gm samples were chemically processed according to the technique of Green (2001) and Chen et al. (2003). The slides containing the radiolarians were studied under Olympus BX 50 Light Microscope and photographed by DP 26 Olympus Digital Camera (Cell Sens Standard) attached to the microscope. In most of the cases, at least 300 radiolarians were counted from each sample; however, in some instances the radiolarians are poorly preserved due to which the number of counted specimens is low. All the figured slides are housed in the repository of Birbal Sahni Institute of Palaeosciences (BSIP), Lucknow, India.

The diversity analysis has been performed using the software PRIMER 5.2.2 (Clarke and Gorley 2001). To figure out Shannon Diversity Index, Simpson Index, Margalef Richness and Pielou's Evenness for each outcrop, the diversity analysis was carried out. To provide an eclectic depiction of diversity patterns, graphs were plotted using Origin Pro 8.0 software (OriginLab Corporation USA 2007).

Water Depth Ecology index (WADE) for each outcrop has been derived from the ratio between the sum of warm-water taxa (i.e., percent of assemblage) and the sum of intermediate (i.e., deeper water) taxa as proposed by Lazarus et al. (2006). Origin Pro 8.0 software has also been used for the graphical representation of the WADE index. The data relating to the ecology of radiolarians have been collected from the published literature. In addition, the database available on the website of Pangea ([www.pangaea.de](http://www.pangaea.de)) and [www.gbif.org](http://www.gbif.org) were taken into consideration for the interpretation of ecological preferences of radiolarian taxa known from different Ocean Drilling Program (ODP), Deep Sea Drilling Program (DSDP), and International Ocean Discovery Program (IODP). Only the taxa identified up to species level have been considered for the WADE analysis. The ecological parameters of only 39 species from the Kalapathar Section, 51 species from the South Point Section, and 46 species from the Laccam Point Section have been taken into consideration following WADE analysis.

## RESULTS

### Radiolarian fauna, events and identified zones

Samples from the Kalapathar Section (BSIP sample nos. 8393/01 to 8393/22) yielded moderately preserved 75 radiolarian taxa belonging to 46 genera, in addition 2 radiolarian forms have been identified only upto the family level (Table 1). The significant and dominant species in this assemblage are: *Calocycletta costata* (8.2%), *Tetrapyle octacantha* (7.4%), *Botryocyrtis suctum* (4.7%), *Liriospyris parkerae* (2.4%), *Didymocyrtis mammifera* (2.3%), *Liriospyris mutuaria* (2.2%),

*Carpocanarium papillosum* (2%), *Liriospyris globosa* (1.6%) etc. The rest of the taxa are listed in Table 1, where the absolute count of all taxa is provided. In addition, some unidentified radiolarians belonging to Spumellaria are also fairly common (Table 1). The generic assignment of these forms is constrained due to preservation potential.

The radiolarian taxa from the South Point Section (BSIP sample nos. 8902/01 to 8902/30) are moderately preserved. Ninety two taxa belonging to 59 genera have been identified from this section, however, 3 radiolarian forms are identifiable only up to the family (Table 2). The dominant species in this assemblage are represented by *Styloclista tenuispina* (8.3%), *Siphocampe lineata* (8.2%), *Calocycletta costata* (7.8%), *Tetrapyle octacantha* (4%), *Styloclista validispina* (3.4%), *Didymocyrtis mammifera* (2.2%), *Liriospyris parkerae* (1.7%), *Heliodiscus echiniscus* (1.6%), *Liriospyris mutuaria* (1.3%), *Liriospyris globosa* (1.1%) etc. In addition, the other recorded taxa from the South Point Section are incorporated in Table 2 that includes unidentified forms belonging to Nassellaria and Spumellaria.

The Laccam Point Section (BSIP sample nos. 8394/01 to 8394/11) also yielded poor to moderately preserved radiolarians assignable to 92 taxa belonging to 54 genera along with 4 radiolarian forms which are identifiable up to the family (Table 3). Significant species preponderant in this section are *Siphocampe lineata* (4%), *Calocycletta costata* (3.8%), *Styloclista tenuispina* (3.5%), *Phormostichoartus marylandicus* (2.7%), *Tetrapyle octacantha* (1.7%), *Liriospyris mutuaria* (1.2%) etc. The absolute count of all the radiolarian species along with other taxa and the unidentified Nassellarian and Spumellarian forms are listed in Table 3.

Significant radiolarian taxa recorded from the above three outcrops of Havelock Island have been documented in Plate 1A-X and Plate 2A-W that show the variations in preservation potential and diversity.

The Kalapathar Section and the lower part of the South Point Section (BSIP sample nos. 8902/30 to 8902/16) are assignable to the *Calocycletta costata* Zone, i.e., RN4 Zone (Sanfilippo and Nigrini 1998) based on the First Occurrence (FO) of *C. costata* and absence of *Dorcadospyris alata* (text-fig. 3). This zone is characterized by the FO of *Carpocanopsis cristatum*, *C. costata* (Nigrini and Sanfilippo 2001), and Last Occurrence (LO) of *Dorcadospyris dentata*, *Didymocyrtis prismatica*, *Peripheraena decora* (Kamikuri et al. 2009a). In both outcrops, *C. costata* is present right at the base (BSIP sample no. 8393/22; 8902/30). Apart from that, the index species stated above are present in both aforementioned outcrops, however, the exact FO and LO of those index species in the outcrops are indiscernible.

The RN4 Zone is considered as the *Calocycletta costata* Zone (Riedel and Sanfilippo 1970, 1978). The top of this zone has been defined by an evolutionary transition from *Dorcadospyris dentata* to *Dorcadospyris alata* that coincides with the lower limit of the *Dorcadospyris alata* Zone, and the base has been defined by the morphotypic lowest occurrence of *C. costata* that coincides with the upper limit of the *Stichocorys wolfii* Zone (Sanfilippo and Nigrini 1998). This zonal scheme for radiolarian biostratigraphy proposed by Sanfilippo and Nigrini (1998) is applicable to tropical low latitudes (Kamikuri et al. 2009a). Due to the presence of *C. costata* and absence of *D. alata* from the base to the top of the Kalapathar Section, it can be assigned to RN4 Zone (text-fig. 3). *Calocycletta costata* is

TABLE 1. Order, preservation potential and occurrence of radiolarian taxa from the Kalapathar Section of Havelock Island (N=Nassellaria and S=Spumellaria)

TABLE 1 – *Continued.*

Radiolarian	Taxa	Sample (8393/)	Order	01	02	03	04	05	06	07	08	09	10	11	12	13	14	15	16	17	18	19	20	21	22
		Preservation	M	M	P	P	M	P	P	M	P	M	M	P	P	M	P	M	M	P	P	P	P	P	
<i>Dendrospyris brusa</i> Sanfilippo and Riedel	N	8	8	0	6	4	4	0	6	0	0	0	0	5	6	10	0	4	2	0	26	0	0	0	
<i>Dendrospyris</i> sp.	N	0	2	4	0	0	0	0	2	0	0	7	5	2	2	4	2	0	0	6	3	0	0	0	
<i>Didymocrytis mammifera</i> Haeckel	S	10	10	6	6	0	8	0	8	6	0	0	7	10	10	10	4	0	4	4	7	12	32		
<i>Didymocrytis prismatica</i> Haeckel	S	2	4	4	0	0	0	0	0	0	0	0	0	0	0	0	0	0	0	0	0	0	0	0	
<i>Dorcadospyris dentata</i> Haeckel	N	0	2	0	0	0	0	2	0	2	0	0	0	0	0	0	0	0	0	0	0	0	0	0	
<i>Druppairactus irregularis</i> Popofsky	S	0	0	0	0	0	0	0	0	0	0	0	0	0	0	0	0	0	0	0	0	0	0	0	
<i>Euchitionia</i> sp.	S	2	0	0	0	0	0	0	0	0	0	0	0	0	0	0	0	0	0	2	0	0	0	3	0
<i>Eucyrtidium hexagonatum</i>																				2	0	0	0	0	
<i>Giraffospyris toxaria</i> Haeckel	N	0	0	3	0	0	0	0	0	0	0	0	0	0	0	0	0	0	0	0	0	0	0	0	
<i>Heliodiscus echiniscus</i> Haeckel	S	2	0	4	0	4	0	0	2	0	0	14	0	0	2	4	4	0	0	7	0	4			
<i>Heliodiscus</i> sp.	S	0	0	0	0	4	0	4	2	0	0	0	0	0	0	0	0	0	0	2	0	0	0	0	
<i>Hexapyle dodecaantha</i> Haeckel	S	2	0	0	0	0	0	0	2	0	0	0	0	0	0	0	0	0	0	0	0	0	0	0	
<i>Hexapyle</i> sp.	S	0	0	0	0	0	0	0	0	0	0	0	0	0	0	0	0	0	4	2	2	0	0	0	
<i>Larcopyle polyacantha?</i>	S	34	16	10	9	16	20	8	26	20	0	0	0	5	4	48	4	16	6	8	0	0	8		
<i>Larcopyle</i> sp.	S	0	4	0	0	2	0	2	4	2	16	0	0	0	2	2	0	4	0	0	0	9	8		
<i>Larcospira</i> sp.	S	0	0	0	0	4	0	0	0	0	0	0	0	0	0	0	0	0	0	0	0	0	0	0	
<i>Liriopsis elevata</i> Goll	N	0	0	0	0	0	0	9	0	0	2	0	0	8	3	0	10	0	0	0	0	0	0	0	
<i>Liriopsis globosa</i> Goll	N	3	0	8	0	0	8	0	0	0	0	2	21	0	3	3	0	10	5	0	19	0	24		
<i>Liriopsis muttaria</i> Goll	N	8	6	8	3	9	8	0	20	0	0	2	0	15	3	16	16	10	5	0	0	6	12		
<i>Liriopsis parkeriae</i> Riedel and Sanfilippo	N	3	12	0	3	9	0	32	11	4	16	2	7	0	10	8	0	32	10	0	0	0	0	0	
<i>Lithomelissa</i> sp.	N	32	0	10	18	4	16	18	42	32	48	32	0	10	6	12	8	8	4	4	0	0	0	0	
<i>Lychnocanium</i> sp.	N	0	0	0	0	0	0	0	0	0	0	0	0	0	4	0	0	2	0	0	0	0	0	0	
<i>Phormospyris</i> sp.	N	0	4	2	6	0	0	4	0	0	0	0	0	0	2	12	4	2	2	4	7	0	0	0	
<i>Phormostichoartius marylandicus</i> Martin	N	2	10	4	0	6	0	0	2	2	0	0	0	0	6	6	4	4	4	8	33	33	4		
<i>Phormostichoartus doliodum</i> Riedel and Sanfilippo	N	0	0	8	0	0	0	4	8	0	0	0	0	15	4	30	0	6	0	0	0	3	0		
<i>Phormostichoartus</i> sp.	N																								

TABLE 1 – *Continued.*

Radiolarian Taxa	Sample (8393/)	01	02	03	04	05	06	07	08	09	10	11	12	13	14	15	16	17	18	19	20	21	22
	Preservation	M	M	P	P	M	P	M	P	M	P	M	P	M	P	M	P	M	P	M	P	P	P
	Order																						
<i>Sethoconus</i> sp.	N	0	0	0	0	0	0	0	0	0	0	0	0	0	0	0	0	0	0	0	0	0	0
<i>Siphocampe lineata</i>	N	2	6	2	3	6	0	0	4	0	0	0	0	0	0	0	2	0	2	0	0	0	6
<i>Siphocampe</i> sp.	N	0	0	0	0	0	0	2	0	0	0	0	0	0	0	4	4	0	4	0	0	0	0
<i>Siphonosphaera</i> sp.	S	0	2	2	0	0	0	0	0	0	0	0	0	0	0	0	2	0	0	0	0	0	0
<i>Solenosphaera zanguebarica</i> Brandt	N	0	2	0	0	0	0	0	0	0	0	0	0	0	0	0	0	0	0	0	0	0	0
<i>Sphaerostylus cristatus</i> Blueford	S	0	0	0	0	8	0	0	0	0	0	0	0	0	0	28	5	6	0	0	0	0	0
<i>Spongodiscus</i> spp.	S	16	32	0	6	8	0	6	10	4	0	0	0	5	4	26	8	0	4	0	0	6	8
<i>Spumellaria</i> gen. and sp. unidentified	S	40	42	26	27	22	56	8	38	40	16	72	0	35	26	48	8	24	36	68	13	0	4
<i>Stichocorys delmontensis</i> Campbell and Clark	N	2	0	0	0	0	0	2	14	2	0	0	0	0	0	2	2	0	0	0	0	3	0
<i>Stichocorys</i> sp.	N	26	2	8	0	10	8	14	18	2	0	24	63	10	22	12	16	10	6	0	0	18	16
<i>Styliaractus universus</i> Hays	S	2	0	0	0	0	0	0	0	0	0	0	0	0	0	0	0	0	0	0	0	0	0
<i>Styliaractus santeamae</i> Campbell and Clark	S	0	2	0	0	0	0	2	0	0	0	0	0	0	0	2	0	0	0	0	0	4	0
<i>Styliaractus</i> sp.	S	0	0	0	0	0	4	0	2	2	0	0	14	0	2	0	0	0	0	0	0	0	0
<i>Styliodictya</i> sp.	S	0	0	3	8	0	2	6	0	0	0	0	5	2	2	4	0	6	0	0	0	3	0
<i>Styliodictya tenuispina</i> Jørgensen	S	10	12	2	6	2	0	2	8	2	0	0	7	5	0	18	0	0	0	20	0	0	0
<i>Styliodictya validispina</i> Jørgensen	S	0	0	0	2	0	0	2	0	0	0	0	0	0	0	2	0	0	0	0	0	0	0
<i>Stylosphaera radiosa?</i> Ehrenberg,	S	2	0	0	0	0	0	0	0	0	0	0	0	7	0	0	4	0	4	2	0	0	0
<i>Stylosphaera</i> sp.	S	0	0	0	0	0	0	0	0	0	0	0	0	0	0	0	0	0	0	0	0	0	0
<i>Tetrapyle octacantha</i> Müller	S	68	32	26	45	36	48	36	54	50	16	0	0	30	14	4	0	2	12	16	0	0	0
<i>Tetrapyle</i> sp.	S	0	2	0	0	8	0	0	6	2	0	0	0	0	2	24	0	2	6	0	0	0	0
<i>Theocorys</i> sp.	N	0	0	4	0	0	8	0	0	0	0	0	0	0	0	4	0	0	0	0	0	0	8
<i>Tholonid</i> sp.	S	0	2	2	0	2	0	0	2	0	0	0	0	0	0	0	0	0	0	0	0	0	0
<i>Tholospyris</i> sp.	N	12	4	16	3	2	8	4	2	6	0	40	14	5	12	6	16	6	8	4	19	6	12
Trissocyclidae	N	4	6	6	3	2	0	12	30	2	0	0	0	10	12	22	8	2	4	12	0	9	4
<i>Tympanidium binoculum</i> Haeckel	N	6	0	0	0	2	0	0	6	6	0	0	0	0	0	0	0	0	0	0	6	8	
<i>Zygocircus</i> sp.	N	6	2	0	3	2	0	4	12	14	0	0	5	6	2	0	12	4	8	0	3	8	
Total		390	346	256	246	284	272	248	494	284	256	494	284	248	245	275	340	548	252	312	288	272	

TABLE 2 – Order, preservation potential and occurrence of radiolarian taxa from the South Point Section of Havelock Island (N=Nassellaria and S=Spumellaria)

TABLE 2—Continued.

Taxa	Preservation Order	Sample (89012)		01	02	03	04	05	06	07	08	09	10	11	12	13	14	15	16	17	18	19	20	21	22	23	24	25	26	27	28	29	30
		P	M	M	M	M	M	M	M	M	M	M	M	M	M	M	M	M	M	M	M	M	M	M	M	M	M	M	M	M	M		
<i>Ciliatirocytus</i> sp.	N	0	0	0	0	0	0	0	0	0	0	0	0	0	0	0	0	0	0	0	0	0	0	0	0	0	0	0	0	0	0		
<i>Collophlaeura</i>	S	3	0	0	0	0	0	0	0	0	0	0	0	0	0	0	0	0	0	0	0	0	0	0	0	0	0	0	0	0	0		
<i>Popofskya</i>																																	
<i>Comella</i>	N	0	0	0	0	0	0	0	0	0	0	0	0	0	0	0	0	0	0	0	0	0	0	0	0	0	0	0	0	0	0		
<i>profunda</i>																																	
Ehrenberg																																	
<i>Cyrtocapsella</i>	N	0	0	0	0	0	0	0	0	0	0	0	0	0	0	0	0	0	0	0	0	0	0	0	0	0	0	0	0	0	0		
<i>comta</i> Haeckel																																	
<i>Cyrtocapsella</i>	N	0	0	0	0	0	0	0	0	0	0	0	0	0	0	0	0	0	0	0	0	0	0	0	0	0	0	0	0	0	0		
<i>tomentosa</i> Haeckel																																	
<i>Dendrocypris</i>	N	0	2	39	0	0	12	6	0	4	0	0	0	0	0	18	4	0	5	0	4	0	0	0	0	0	0	0	0	0			
<i>bursa</i> Santillopo and Riedel																																	
<i>Dendrocypris</i>	N	0	0	0	0	0	0	0	0	0	0	0	0	0	0	0	0	0	0	0	0	0	0	0	0	0	0	0	0	0	0		
<i>podocladus</i>																																	
Carevale																																	
<i>Dendrocypris</i> sp.	N	0	0	4	0	0	0	0	0	0	0	0	0	0	0	0	2	0	0	0	2	0	0	0	0	0	0	0	0	0	0		
<i>Didymocystis</i>	S	0	0	0	0	0	0	0	0	0	0	0	0	0	0	0	0	0	0	0	0	0	0	0	0	0	0	0	0	0	0		
<i>basimii</i> Carevale																																	
<i>Didymocystis</i>	S	0	0	0	0	0	0	0	0	0	0	0	0	0	0	0	0	0	0	0	0	0	0	0	0	0	0	0	0	0	0		
<i>latifrons</i> Riedel																																	
<i>Diatomocystis</i>	S	7	6	8	0	4	9	14	16	8	6	18	5	4	12	5	0	4	0	6	0	11	0	6	36	10	12	4	0	4			
<i>mammifera</i>																																	
Haeckel																																	
<i>Didymocystis</i> sp.	N	0	0	0	0	0	0	3	2	0	0	0	0	0	0	0	0	0	0	0	0	0	0	0	0	0	0	0	0	0	0		
<i>Dorcatoma</i> sp.																																	
<i>ata</i> Riedel																																	
<i>Drepanoceras irregularis</i>	S	0	2	0	0	0	0	0	0	0	0	0	0	0	0	0	2	0	0	0	0	0	0	0	0	0	0	0	0	0	0		
<i>Eucypris</i>	N	0	0	0	0	0	0	0	0	0	0	0	0	0	0	0	0	0	0	0	0	0	0	0	0	0	0	0	0	0	0		
<i>histicornis</i>																																	
Hilsemann																																	
<i>Eucyrtidium</i>	N	0	0	8	0	0	0	0	0	0	0	0	0	0	0	0	2	0	0	4	0	0	0	0	0	0	0	0	0	0	0		
<i>punctatum?</i>																																	
Ehrenberg																																	
<i>Ginolfopyris</i>	N	0	0	0	0	0	0	0	0	0	0	0	0	0	0	0	0	0	0	0	0	0	0	0	0	0	0	0	0	0	0		
<i>taxaria</i> Haeckel	S	0	2	8	0	12	6	6	20	6	2	6	0	8	4	24	0	0	4	0	0	6	2	0	0	6	4	15	4	4			
<i>Helicidius</i>																																	
<i>orbicularis</i>																																	
Haeckel																																	
<i>Hexactinum</i>	S	0	0	0	0	0	0	0	0	0	0	0	0	0	0	0	2	0	0	0	0	0	0	0	0	0	0	0	0	0	0		
<i>pachidernum</i>																																	
Jørgensen																																	
<i>Hexapyle</i>																																	
<i>dodecandra</i>																																	
Haeckel																																	
<i>hexastylius</i>	S	0	2	0	0	8	0	0	0	0	0	0	0	0	0	0	0	2	4	0	0	0	0	0	0	0	7	0	0	0	0		
<i>dimensions</i>																																	
Haeckel																																	
<i>Lamprocydas</i>	N	0	0	0	0	0	0	0	0	0	0	0	0	0	0	0	0	0	0	0	0	0	0	0	0	0	0	0	0	0	0		
<i>mangostensis</i>																																	
Campbell and Clark																																	
<i>Larcepole</i>																																	
<i>nebulosum Lazarus et al.</i>	S	0	0	0	0	0	0	0	0	0	0	0	0	0	0	0	0	0	0	0	0	0	0	0	0	0	0	0	0	0	0		

TABLE 2—Continued.

TABLE 2—Continued.

Radiolarian	Sample (8902)	01	02	03	04	05	06	07	08	09	10	11	12	13	14	15	16	17	18	19	20	21	22	23	24	25	26	27	28	29	30	
Taxa	Preservation Order	P	M	P	M	M	P	M	M	M	P	M	M	P	M	M	P	P	P	P	P	P	P	P	P	P	P	P	M			
<i>Silicicorvus</i>	N	0	0	0	0	0	0	2	4	0	0	0	0	0	0	4	0	0	3	0	11	0	0	0	0	4	0	4	0			
<i>deltamonensis</i>	Campbell and Clark																															
<i>Silicicorvus</i> sp.	N	31	12	26	24	52	30	44	40	46	54	24	19	38	44	24	46	42	32	36	17	0	33	29	27	44	30	20	24	42	40	
<i>Syllicorvus</i>	S	0	0	0	0	6	0	0	0	0	2	0	0	2	2	4	0	3	0	0	0	0	3	4	0	4	10	0	8			
<i>Syllicorvus</i>	S	0	0	0	0	0	0	0	4	0	0	0	0	0	0	0	0	0	0	0	0	0	0	0	0	0	0	0	0			
<i>Syllicorvus</i>	S	0	2	0	3	0	0	0	0	0	0	2	0	9	2	4	0	0	2	9	0	2	5	0	0	0	0	0	0			
<i>Syllicorvus</i> sp.	S	24	40	0	27	18	54	40	56	32	30	15	48	62	32	10	26	25	34	27	37	2	72	4	21	28	0	0	28	38	32	
<i>Sylocidicyva</i>	Jorgensen	S	14	12	0	12	22	12	28	16	18	12	33	0	20	8	10	10	16	32	0	0	0	0	0	0	0	0	0	4	8	
<i>Sylocidicyva</i>																																
<i>Sylocidicyva</i>	Jorgensen	S	0	0	0	0	0	0	0	0	0	0	2	3	0	0	0	2	0	0	0	0	0	0	0	0	0	0	0	0		
<i>Sylocidicyva</i>	Jorgensen	S	3	2	0	6	8	0	4	4	0	4	3	4	4	4	2	0	2	6	4	0	0	0	0	0	0	0	0	0		
<i>Sylocidicyva</i>	Ehrenberg	S	17	24	9	24	16	30	10	32	10	8	0	14	46	18	8	10	25	8	0	6	0	11	22	15	0	0	12	4	25	8
<i>Sylocidicyva</i>	Tenpyle Müller	S	0	0	0	0	0	0	0	0	0	0	0	0	0	0	0	0	0	0	0	0	0	0	0	0	0	0	0	0		
<i>Theocidicyva</i> sp.	N	0	0	0	0	4	0	0	0	0	0	0	0	0	0	0	4	2	0	0	0	5	4	0	0	0	0	0	0	0	0	
<i>Theocidicyva</i> sp.	N	0	0	0	0	12	0	6	2	0	4	0	0	4	0	0	0	0	0	0	0	0	0	0	0	0	0	0	0	0		
<i>Thalidopsis</i>	N	0	2	0	18	16	0	8	4	6	10	0	14	32	6	0	0	0	0	3	0	0	7	12	4	5	0	4	0	0		
<i>Thalidopsis</i>	N	3	24	9	12	8	6	0	8	2	0	0	0	19	6	6	0	0	8	14	3	0	6	0	6	4	5	8	5	13	8	
<i>Trisicyclidae</i>	N	3	2	0	0	0	0	0	0	0	2	6	5	4	2	0	10	5	4	0	0	22	0	6	0	0	0	0	0	0	4	
<i>Tympanidium</i>																																
<i>Tympanidium</i>																																
<i>bimaculum</i>	Haeckel	N	0	14	9	12	12	0	0	8	10	4	6	0	14	22	8	5	3	0	0	7	0	6	7	0	4	0	0	5	9	
<i>Zigocircus</i> sp.																																
Total		321	338	309	348	356	324	436	472	402	356	336	312	504	446	360	340	381	444	308	312	8	302	335	333	308	305	320	301	304	368	

TABLE 3  
Order, preservation potential and occurrence of radiolarian taxa from the Laccam Point Section of Havelock Island (N=Nassellaria and S=Spumellaria).

Radiolarian Taxa	Sample (8394/) Preservation Order	01 M	02 P	03 M	04 M	05 P	06 M	07 P	08 P	09 P	10 P	11 M
<i>Acrobotrys cribosa</i> Popofsky	N	1	3	6	6	0	0	9	8	2	0	0
<i>Acrobotrys disolenia</i> Haeckel	N	0	0	0	0	0	0	0	0	0	0	0
<i>Acrosphaera spinosa</i> Haeckel	S	0	0	0	0	0	0	0	0	0	0	0
<i>Actinomma medusa?</i> Ehrenberg	S	0	11	4	2	0	0	0	0	0	0	0
<i>Actinomma</i> sp.	S	1	3	0	2	0	3	0	0	2	3	1
<i>Actinommidae</i>	S	0	4	3	2	0	0	0	4	2	0	0
<i>Albatrossidium</i> sp.	N	0	4	0	0	0	0	0	0	0	0	0
<i>Amphistylus angelinus</i> Campbell and Clark	S	0	0	0	0	0	0	1	8	4	4	0
<i>Amphistylus angelinus?</i> Campbell and Clark	S	6	3	1	2	0	3	0	0	2	0	0
<i>Amphistylus</i> sp.	S	0	0	0	2	0	2	3	0	0	0	0
<i>Artostrobium</i> sp.	N	0	0	2	2	0	0	0	0	0	0	0
<i>Artostrobus annulatus</i> Bailey	N	2	3	2	0	0	0	7	0	0	3	3
<i>Artostrobus</i> sp.	N	1	3	0	0	0	0	0	0	0	0	0
<i>Botryocyrtis scutum</i> Harting	N	10	3	6	8	5	5	1	12	6	0	4
<i>Calocycletta costata</i> Riedel and Sanfilippo	N	12	10	25	10	6	13	11	4	0	12	23
<i>Calocycletta robusta</i> Moore	N	2	0	1	6	0	1	0	0	0	1	0
<i>Calocycletta</i> sp.	N	3	0	3	2	0	2	2	0	0	6	6
<i>Carpocanarium aff. papillosum</i>	N	5	7	16	4	0	3	10	0	6	14	0
<i>Carpocanarium papillosum</i>												
Ehrenberg	N	3	3	1	4	0	1	4	0	4	2	3
<i>Carpocanarium</i> sp.	N	0	0	1	4	5	4	3	0	0	11	0
<i>Carpocaniidae</i>	N	0	0	0	2	0	2	0	0	0	0	0
<i>Carpocanium kinugasense</i>												
Nishimura	N	3	0	4	2	0	2	3	0	4	0	1
<i>Carpocanium</i> sp.	N	0	0	1	0	0	2	3	0	4	0	7
<i>Carpocanopsis</i> sp.	N	1	3	1	4	0	0	0	0	2	0	1
<i>Carpocanopsis cristatum</i>												
Carnevale	N	6	0	3	0	0	7	0	0	13	6	6
<i>Carposphaera</i> sp.	S	0	3	1	4	0	2	1	4	0	2	1

also present and *D. alata* is also absent at the base of the South Point Section, so the lower part of South Point Section (BSIP sample nos. 8902/30 to 8902/16) is assignable to RN4 Zone (text-fig. 3).

The upper part of the South Point Section (BSIP sample nos. 8902/15 to sample no. 8902/01) and the entire Laccam Point Section (BSIP sample nos. 8394/11 to 8394/01) have been assigned to RN5 Zone i.e., *Dorcadospyris alata* Zone due to the FO of *D. alata* (text-fig. 3) in both the sections. There are number of radiolarian events within the RN5 Zone however, some important events are marked by FOs of *Dorcadospyris alata*, *Didymocystis laticonus*, *Lithopera thornburgi* (Kamikuri et al. 2009a) and LOs of *Dendrospyris bursa*, *D. mammifera*, *D. basanii* (Kamikuri et al. 2009a), *C. costata* (Nigrini and Sanfilippo 2001; Kamikuri et al. 2009a), *C. robusta* (Kamikuri et al. 2009a), *Liriospyris parkerae* (Nigrini and Sanfilippo 2001; Kamikuri et al. 2009a). In the radiolarian assemblage of this zone all the index species cited above commonly occur in both South Point and Laccam Point sections. It should be mentioned that the lower boundary of the *Dorcadospyris alata* Zone (RN5) is defined by the evolutionary transition (ET) of *D. alata* from *D. dentata* (Sharma et al. 2011). However, according to Sharma and Devi (2007), this

event is not applicable in the Andaman-Nicobar Basin as both these species are extremely rare. Therefore, morphotypic FO of *D. alata* is used to define the lower boundary of the RN5 Zone (Sharma et al. 2011). In the present study from the South Point and Laccam Point sections, both the radiolarian species are present.

The RN5 Zone is defined as the *Dorcadospyris alata* Zone (Riedel and Sanfilippo 1970; 1971; 1978). Sanfilippo and Nigrini (1998) designated the top of this zone by the morphotypic lowest occurrence of *Diartus petterssoni*, but Johnson and Nigrini (1985) considered it as a diachronous event that coincides with the lower limit of the *Diartus petterssoni* Zone. The base of the RN5 Zone is defined by the evolutionary transition from *D. dentata* to *D. alata* that coincides with the upper limit of the *Calocycletta costata* Zone (Sanfilippo and Nigrini 1998). In the South Point Section, the FO of *D. alata* in BSIP sample no. 8902/15 indicates that the upper part of the section belongs to the RN5 Zone i.e., *Dorcadospyris alata* Zone (text-fig. 3). In the Laccam Point Section, *D. alata* is present from the base and continues to the top. So, the Laccam Point Section can be assigned to the RN5 Zone (text-fig. 3). However, one significant finding in this section is the presence of *L. thornburgi* in the top-most sample (BSIP sample no. 8394/01).

TABLE 3  
Continued.

Radiolarian Taxa	Sample (8394/) Preservation Order	01 M 02 P 03 M 04 M 05 P 06 M 07 P 08 P 09 P 10 P 11 M																					
		01 M		02 P		03 M		04 M		05 P		06 M		07 P		08 P		09 P		10 P		11 M	
		01	M	02	P	03	M	04	M	05	P	06	M	07	P	08	P	09	P	10	P	11	M
<i>Cenosphaera</i> sp.	S	0	0	0	0	0	0	2	0	0	0	6	0	0	0	0	0	0	0	0	0	0	0
<i>Ceratocyrtis</i> sp.	N	0	0	0	0	0	0	0	0	0	2	0	0	0	0	0	0	0	0	0	0	0	0
<i>Circodiscus</i> spp.	S	3	0	0	0	0	0	0	0	0	1	0	0	0	0	0	0	0	0	0	0	0	9
<i>Clathrocanium</i> sp.	N	0	0	0	0	2	0	2	0	0	0	0	0	0	0	0	0	0	0	0	0	0	0
<i>Clathrocanium</i> <i>sphaerocephalum</i> Haeckel	N	0	0	0	0	0	0	0	0	0	1	0	0	0	0	0	0	0	0	0	0	0	0
<i>Collosphaera brattstroemi</i>																							
Bjorklund and Goll	S	0	0	0	0	0	0	0	0	0	0	0	0	0	0	0	0	0	0	0	0	0	1
<i>Collosphaera macropora</i>																							
Popofsky	S	0	0	1	0	0	0	2	0	0	0	0	0	0	0	0	0	0	0	0	0	0	1
<i>Cornutella profunda</i> Ehrenberg	N	0	3	0	2	0	0	0	0	0	0	0	0	0	0	0	4	6	3				
<i>Cyrtocapsella cornuta</i> Haeckel	N	0	0	0	0	0	0	0	0	0	1	0	0	0	0	0	0	0	0	0	0	0	0
<i>Cyrtocapsella tetraptera</i> Haeckel	N	0	0	0	2	0	0	0	0	0	0	0	0	0	0	0	0	0	0	0	0	0	0
<i>Dendrosprysis bursa</i> Sanfilippo and Riedel	N	0	0	3	0	0	0	0	0	0	0	0	0	0	0	0	0	0	2	0	0	0	0
<i>Dendrosprysis</i> sp.	N	0	0	0	4	6	9	2	0	0	0	0	0	0	0	0	0	2	1				
<i>Didymocystis mammifera</i>																							
Haeckel	S	1	0	0	4	0	1	2	4	2	0	0	0	0	0	0	0	0	0	0	0	0	0
<i>Didymocystis</i> sp.	S	1	0	7	4	0	3	3	4	2	8	0	0	0	0	0	0	0	0	0	0	0	0
<i>Dorcadosprys alata</i> Riedel	N	4	7	7	4	0	0	3	0	0	2	1	1	0	0	0	0	2	1				
<i>Druppatractus nanus</i> Blueford	S	3	0	0	0	0	0	2	0	4	0	0	0	0	0	0	0	0	0	0	0	0	0
<i>Druppatractus</i> sp.	S	1	0	0	0	6	2	3	0	0	0	0	0	0	0	0	0	0	0	0	0	0	0
<i>Euchitonita</i> sp.	S	0	0	3	2	0	0	0	0	0	0	0	0	0	0	0	0	0	2	0	0	0	0
<i>Eucyrtidium hexagonatum</i>																							
Haeckel	N	0	0	3	2	0	2	2	0	0	0	0	0	0	0	0	0	0	0	0	0	0	0
<i>Eucyrtidium</i> sp.	N	1	0	12	2	0	1	3	0	0	4	1	1	1	1								
<i>Heliodiscus echiniscus</i> Haeckel	S	1	0	9	0	0	0	6	0	0	0	0	0	0	0	0	0	0	0	0	0	0	0
<i>Heliodiscus</i> sp.	S	3	0	4	4	5	1	0	0	0	0	2	6	3									

#### New record of radiolarian species from the northeastern part of the Indian Ocean

Four species of radiolarians have been identified in the present study, though most of the species are sporadically present in few samples of the three studied sections. These four species were not recorded earlier from the northeastern part of the Indian Ocean. These species are:

*Eucecryphalus histricosus* Hülsemann- It is characterized by the presence of cephalis with a distinct apical horn and slightly constricted thorax with numerous small bristles extended up to the upper part of the thorax (Plate 1X). Numerous unevenly rounded to hexagonal pores are distributed in more or less regular vertical rows, but towards the cephalis, the dimension of the pores decreases.

*Hexacontium pachydermum* Jørgensen- This cosmopolitan species identified in the present study is distinguished by its faint spines on the thick outer shell that consist of more or less rounded pores with strong, long main spines (Plate 2K). However, most of the long main spines are broken.

*Larcopyle pylomaticus* Riedel- In having sub-cylindrical shell with a densely spongy core possessing dark appearance in the inner part, this species is assignable to *Larcopyle pylomaticus*. The spongy outer wall consists of small pores arranged close to-

gether and lack frames with multiple spirals and constantly spaced whorls (Plate 2J).

*Stylodictya tenuispina* Jørgensen- This warm-water species is distinguishable by almost linear, somewhat thicker in the middle and slightly narrowed towards the ends of the shell which is almost round. It possesses almost angular inner rings and regular outer rings (Plate 2F).

#### Diversity analysis

To summarize the diversity of radiolarians in all the three outcrops, Shannon diversity ( $H'$ ), Simpson Index (D), Margalef Richness (d), Number of species (N) and Pielou's Evenness ( $J'$ ) were computed (text-figs. 4A-C). Shannon diversity ( $H'$ ) is defined as the measurement of diversity that combines species richness and their relative abundance, whereas, Simpson Index (D) is the measurement of diversity that takes into account the number of species present as well as relative abundance of each species. Margalef Richness (d) is the count of different species present in an ecological community, and Pielou's Evenness ( $J'$ ) refers to the distribution of abundance across the species in a community.

At the Kalapathar Section,  $H'$  ranges from 2.2 to 3.4 and the number of radiolarian species (S) ranges from 12 to 51 (text-fig. 4A). The lowest diversity ( $H'$ ) was observed in BSIP sample no. 8393/11 and the highest in sample no. 8393/15, which is also evident from Simpson Index (D) (text-fig. 4A). Species Rich-

TABLE 3  
Continued.

Radiolarian Taxa	Sample (8394/) Preservation Order	01 M	02 P	03 M	04 M	05 P	06 M	07 P	08 P	09 P	10 P	11 M
<i>Lamprocyclas margatensis</i>												
Campbell and Clark	N	0	0	1	2	0	0	0	0	0	0	0
<i>Lamprocyclas</i> sp.	N	0	0	0	0	0	0	0	0	2	1	0
<i>Larcopyle nebulum</i> Lazarus												
Faust and Popova-Goll	S	2	0	0	2	0	0	1	4	0	0	0
<i>Larcopyle polycantha?</i>	S	6	3	6	2	0	11	1	4	0	3	3
<i>Larcopyle pylomaticus</i> Riedel	S	0	0	1	0	0	0	0	0	0	0	0
<i>Larcopyle</i> sp.	S	37	28	25	36	22	27	25	28	33	29	39
<i>Larcospira</i> spp.	S	0	0	0	2	0	0	0	0	0	0	0
<i>Liriospyris elevata</i> Goll	N	0	0	9	2	0	0	0	0	0	2	0
<i>Liriospyris globosa</i> Goll	N	0	0	3	0	0	0	13	0	0	1	0
<i>Liriospyris mutuaria</i> Goll	N	0	3	6	4	0	0	0	0	15	0	13
<i>Liriospyris parkerae</i> Riedel and Sanfilippo	N	6	7	1	0	0	0	2	0	0	3	4
<i>Liriospyris</i> spp.	N	7	3	13	8	0	5	10	0	17	33	18
<i>Lithatractus</i> sp.	S	0	0	1	0	0	0	0	0	0	0	0
<i>Lithomelissa</i> sp.	N	5	3	0	8	16	14	4	4	6	1	6
<i>Lithopera thornburgi</i> Sanfilippo and Riedel	N	1	0	0	0	0	0	0	0	0	0	0
Nassel. gen and sp. indet.	N	6	3	4	0	0	5	3	4	0	0	4
<i>Otosphaera polymorpha</i>												
Haeckel	S	1	0	5	2	0	3	1	0	2	6	1
<i>Otosphaera</i> sp.	S	0	0	3	0	0	1	2	0	0	0	0
<i>Peridium</i> sp.	N	0	0	0	0	0	0	1	0	0	0	0
<i>Phormospyris</i> sp.	N	0	0	1	6	5	3	2	4	4	0	2
<i>Phormostichoartus doliolum</i>												
Riedel and Sanfilippo	N	0	0	0	0	0	0	1	0	6	0	9
<i>Phormostichoartus marylandicus</i> Martin	N	4	0	18	8	11	16	15	0	11	0	6
<i>Phormostichoartus</i> sp.	N	9	21	22	8	27	16	15	16	15	14	4
<i>Sethoconus</i> sp.	N	0	3	0	0	0	0	0	0	0	0	0
<i>Siphocampe arachnea</i>												
Ehrenberg	N	0	3	1	0	0	0	4	0	0	0	0

ness, i.e., Margalef Richness (d) varies from 2 to 8. The acme of species richness is in BSIP no. 8393/15 and lowest in BSIP no. 8393/10. Accordingly, the Pielou's Evenness ( $J'$ ) also shows high values (0.95) in BSIP no. 8393/10. The value of evenness varies from 0.80 to 0.95 and as a consequence in BSIP no. 8393/10, the highest value of evenness with the lowest value of Margalef Richness was observed.

The Shannon Diversity analysis reveals that the number of radiolarian species (S) at the South Point Section ranges from 4 to 46 (text-fig. 4B). The Shannon Diversity Index i.e.,  $H'$  ranges from 1.38 to 3.2. In BSIP sample no. 8902/21 the lowest diversity ( $H'$ ) was observed (text-fig. 4B) that is also reflected by Simpson Index. The Margalef Richness (d) varies from 1.4 to 7.3. The lowest value (1.4) of species richness is evident in BSIP sample no. 8902/21. The value of Pielou's Evenness ( $J'$ ) varies from 0.80 to 1. In BSIP sample no. 8902/21;  $J'$  is highest (1), in which the species richness (d) is the lowest (1.4).

The number of radiolarian species (S) at the Laccam Point Section ranges from 21 to 62 as derived from Shannon Diversity analysis (text-fig. 4C). In this section, the value of  $H'$  is the lowest in BSIP sample no. 8394/05 (2.84) and the highest in BSIP sample no. 8394/03 (3.6). The Simpson Index (D) also corroborates with the Shannon Diversity ( $H'$ ). In BSIP sample no.

8394/05, species richness, i.e., Margalef Richness (d) was observed low (3.6) and in BSIP sample no. 8394/03 it was computed highest (10.2). The Pielou's Evenness ( $J'$ ) varies from 0.88 to 0.93, which shows the lowest value in BSIP sample no. 8394/03 and the highest value (0.93) in BSIP sample no. 8394/05. As a consequence, BSIP sample no. 8394/05 recorded the highest value of evenness ( $J'=0.93$ ) with low species richness ( $d=3.64$ ).

#### WADE Index

In the present study, WADE analysis was carried out based on the ecological preferences of the radiolarian species recorded from individual outcrops. In the Kalapathar Section, 23 are warm-water species and 15 are cosmopolitan, whereas in the South Point Section 27 species are warm-water species and 24 species are cosmopolitan (Table 4). However, in the Laccam Point Section, both warm-water and cosmopolitan species are represented by 23 each (Table 4). WADE ratio obtained from the analyses on each outcrop was plotted concerning the samples (text-figs. 5A-C). The WADE ratio indicates that all three sections of the present study are dominated by the warm species. As a result, in all the plots (text-figs. 5A-C) derived by Origin Pro 8.0 software depict the trend lines towards higher values. The WADE ratio in the Kalapathar (text-fig. 5A), South

TABLE 3  
Continued.

Radiolarian Taxa		Sample (8394/) Preservation Order	01 M	02 P	03 M	04 M	05 P	06 M	07 P	08 P	09 P	10 P	11 M
<i>Siphocampe lineata</i> Ehrenberg	N	9	14	19	8	22	11	13	0	8	16	13	
<i>Siphocampe</i> sp.	N	0	0	3	0	5	1	0	4	0	0	0	
<i>Siphonosphaera</i> sp.	S	0	0	0	0	0	0	0	4	0	3	0	
<i>Siphostichoartus corona</i>													
Haeckel	N	0	0	1	0	0	0	0	0	0	0	0	
<i>Spongocore puella</i> Haeckel	S	0	3	0	0	0	0	0	0	0	0	0	
<i>Spongodiscidae</i>	S	2	0	2	0	0	0	0	0	0	0	0	
<i>Spongodiscus</i> sp.	S	80	18	21	34	16	23	22	12	35	10	34	
Spumell. gen and sp. indet.	S	16	10	11	0	16	11	10	16	2	4	16	
<i>Stichocorys delmontensis</i>													
Campbell and Clark	N	0	0	0	0	5	2	0	0	0	0	0	
<i>Stichocorys</i> sp.	N	22	14	25	38	27	29	37	12	35	27	36	
<i>Stichopileum</i> sp.	N	0	0	0	0	0	0	0	0	2	0	0	
<i>Stylatractus santaeannae</i>													
Campbell and Clark	S	0	0	0	0	0	0	0	0	2	3	2	
<i>Stylatractus</i> sp.	S	0	0	3	0	5	7	0	0	0	0	7	
<i>Stylatractus universus</i> Hays	S	0	0	1	0	0	0	0	0	0	0	0	
<i>Stylocidicta</i> sp.	S	11	10	7	4	11	5	0	28	4	11	9	
<i>Stylocidictya tenuispina</i> Jørgensen	S	15	10	18	8	16	20	6	4	6	13	1	
<i>Stylocidictya validispina</i>													
Jørgensen	S	0	0	3	6	0	2	4	4	0	1	0	
<i>Stylosphaera</i> sp.	S	0	0	0	0	0	0	0	0	0	0	0	
<i>Stylosphaera radiosa</i> Ehrenberg	S	0	0	5	4	0	0	0	0	2	0	0	
<i>Tetrapyle octacantha</i> Müller	S	0	3	3	14	5	7	6	8	4	4	3	
<i>Theocorys</i> sp.	N	0	0	0	2	0	0	0	0	0	0	5	
<i>Tholospyris</i> sp.	N	6	7	1	8	0	2	1	0	0	0	0	
<i>Trissocyklidae</i>	N	6	7	5	8	0	7	10	16	13	5	12	
<i>Tympanidium binoctonum</i>													
Haeckel	N	3	0	8	6	0	5	4	0	0	3	4	
<i>Zigocircus</i> sp.	N	4	3	1	10	0	0	0	8	11	2	0	
Total		332	249	387	340	242	312	300	228	306	288	327	

Point (text-fig. 5B), and Laccam Point (text-fig. 5C) sections varies from 7.6 to 0.6, 6.3 to 0.7, and 3.1 to 0.7 respectively. The lowest value of the WADE ratio was noticed in sample no. 8393/09 (0.6) of the Kalapathar Section (text-fig. 5A), in BSIP sample no. 8902/17 (0.7) of the South Point Section (text-fig. 5B), and in BSIP sample no. 8394/08 (0.7) of the Laccam Point Section (text-fig. 5C). As far as, the highest value of the WADE ratio is concerned, in the Kalapathar Section it was observed in BSIP sample no. 8393/17 (7.6), in the South Point Section in BSIP sample no. 8902/26 (6.3) and in the Laccam Point Section in BSIP sample no. 8394/01 (3.1). It should be mentioned here that in both Kalapathar and South Point sections there are discontinuities in the trend lines due to very few occurrence of radiolarians in the respective samples (text-figs. 5A, B). Moreover, these samples (BSIP sample no. 8393/11 in the Kalapathar Section and BSIP sample no. 8902/21 in the South Point Section) are devoid of any cosmopolitan species.

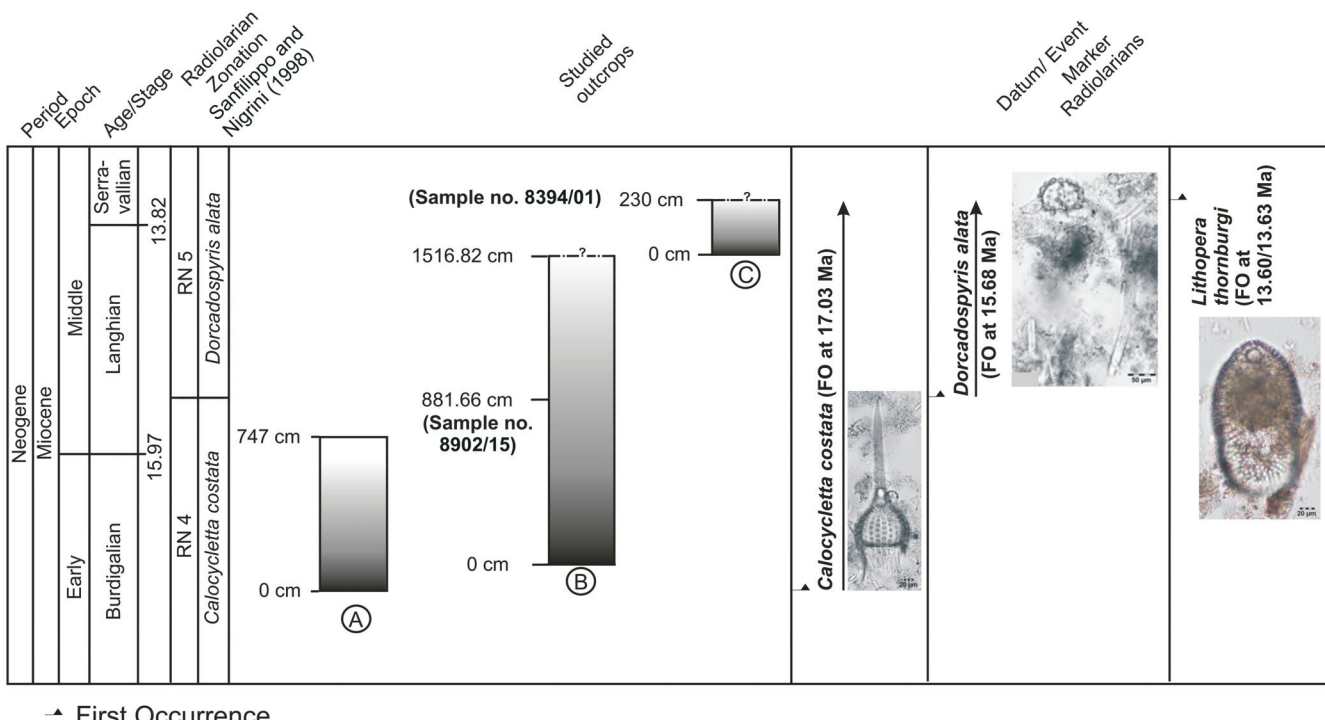
## DISCUSSION

### Age and sedimentation

For determining the radiolarian zones and relative age of the sediments, stratigraphically index species preserved in the rocks play a key role. Specifically for the Neogene sediments of

tropical low latitude, the radiolarian zones proposed by Sanfilippo and Nigrini (1998) are widely applied (Kamikuri et al. 2009a; Zhang et al. 2014; Li et al. 2015).

Within the RN4 Zone, the FO of *Calocycletta costata* has been calibrated as 17.03 Ma from the tropical Pacific, the Indian Ocean as well as the Atlantic Ocean (Sanfilippo and Nigrini 1995) and 17.59 Ma from the South China Sea (Li et al. 2015). The LO of *C. costata* was standardized as 14.74 Ma based on calibrated data from different sites across the globe (Lazarus et al. 1995). Nigrini and Sanfilippo (2001) designated the LO of *C. costata* as 14.5/14.6 Ma and 15.0/15.1 Ma from the western and central Pacific respectively. Later on, its LO has been calibrated 13.63/14.70 Ma from the eastern equatorial Pacific (Kamikuri et al. 2009a) and 15.00 Ma from the South China Sea (Li et al. 2015). The culmination of the RN4 Zone is marked by the FO of *D. alata*, which demarcates the *Dorcadospyris alata* Zone, i.e., the RN 5 Zone (Sanfilippo and Nigrini 1998). Its FO has been calibrated as 15.68 Ma from the tropical Pacific, Indian and Atlantic oceans (Sanfilippo and Nigrini 1995) and 15.36 Ma from different sites across the globe (Lazarus et al. 1995), 14.83/14.99 Ma from the eastern equatorial Pacific (Kamikuri et al. 2009a), 15.03 Ma from the South China Sea (Li et al. 2015). Its LO is at 11.8/12.0 Ma and 13.5/13.7 Ma (Nigrini and



TEXT-FIGURE 3

Columnar representation of the A. Kalapathar Section, B. South Point Section (—?— indicates upper limit not defined), C. Laccam Point Section (—?— indicates upper limit not defined) showing the radiolarian zonations (following Sanfilippo and Nigrini 1998) and relative age based on marker radiolarian species (FO).

Sanfilippo 2001) from the western and central Pacific Oceans respectively, whereas, in the eastern equatorial Pacific Kamikuri et al. (2009a) designated the LO of *D. alata* at 11.77/12.04 Ma.

Based on the foregoing account, a Burdigalian-Langhian stage/age can be assigned for both the Kalapathar Section and lower part of the South Point Section that belongs to the RN Zone. On the other hand, the upper part of the South Point Section and the entire Laccam Point Section contains index species of radiolarians that belong to RN5 Zone. However, one significant finding is the presence of *L. thornburgi* in the topmost sample (8394/01) of the Laccam Point Section that indicates the onset of Serravallian sedimentation. Kamikuri et al. (2009a) suggested that in the eastern equatorial Pacific, the FO of *L. thornburgi* is at 13.60/13.63 Ma that pertains to the Serravallian stage/age (text-fig. 3). Accordingly, the age of the Laccam Point Section may be assigned as the Langhian-Serravallian stage/age. The estimated relative age of the Kalapathar Section owing to presence of *C. costata* and absence of *D. alata* may be designated as <17.03 Ma and >15.68 Ma. Based on the occurrence of *C. costata* and absence of *D. alata* from the base (BSIP sample no. 8902/30) to BSIP sample no. 8902/16 in the South Point Section the relative age may be assigned to <17.03 Ma and >15.68 Ma. On the other hand, owing to the presence of *D. alata* and absence of *L. thornburgi* from BSIP sample no. 8902/15 to the top (BSIP sample no. 8902/01) of the South Point Section, the relative age can be estimated to <15.68 Ma and >13.60/13.63 Ma. The age for youngest outcrop, i.e., the Laccam Point Section, can be estimated as <15.68 Ma and

>13.60/13.63 Ma from the base (BSIP sample no. 8394/11) to the BSIP sample no. 8394/02 due to the presence of *C. costata* and *D. alata* and the topmost strata can be dated as <13.60/13.63 Ma due to presence of *L. thornburgi* in BSIP sample no. 8394/01.

The sedimentation rate during Burdigalian-Langhian time in the Havelock Island has been estimated as ~27 m/Myr based on the identified calcareous nannofossil events in a recent study (Chakraborty et al. 2021) and it was the first attempt for the estimation of sedimentation rate for the late early to early middle Miocene in the northeastern part of the Indian Ocean. In IODP expedition 353 (Clemens et al. 2016), the sedimentation rate for this time slice was not deduced due to the unavailability of significant biostratigraphic events. However, based on available data from the Arabian Sea (NGHP/01A, Kerala Konkan Basin), it is evident that during the early middle Miocene the sedimentation rate was ~25m/Myr (Flores et al. 2014). In the present study in a single outcrop, there is a lack of accurate strata of any two significant radiolarian events (i.e., FO or LO) for determining the sedimentation rate. So, if we consider the nannofossil data recently published from the Havelock Island (Chakraborty et al. 2021), the rate of sedimentation during this time slice was ~27m/Myr.

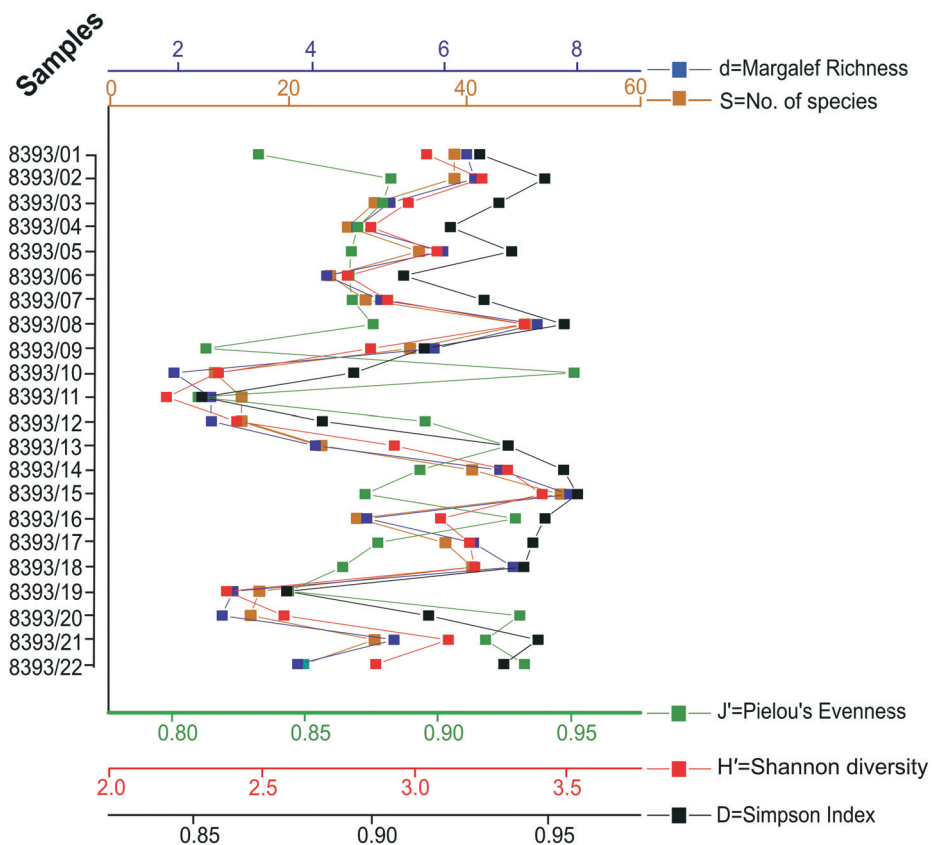
#### Correlation

Several radiolarian taxa recorded herein also have been reported from the late early to early middle Miocene radiolarian assemblages (Table 5) in the DSDP Leg 22 (sites 211, 213, 214, 216) drilled at the eastern part of the Indian Ocean (Johnson 1974),

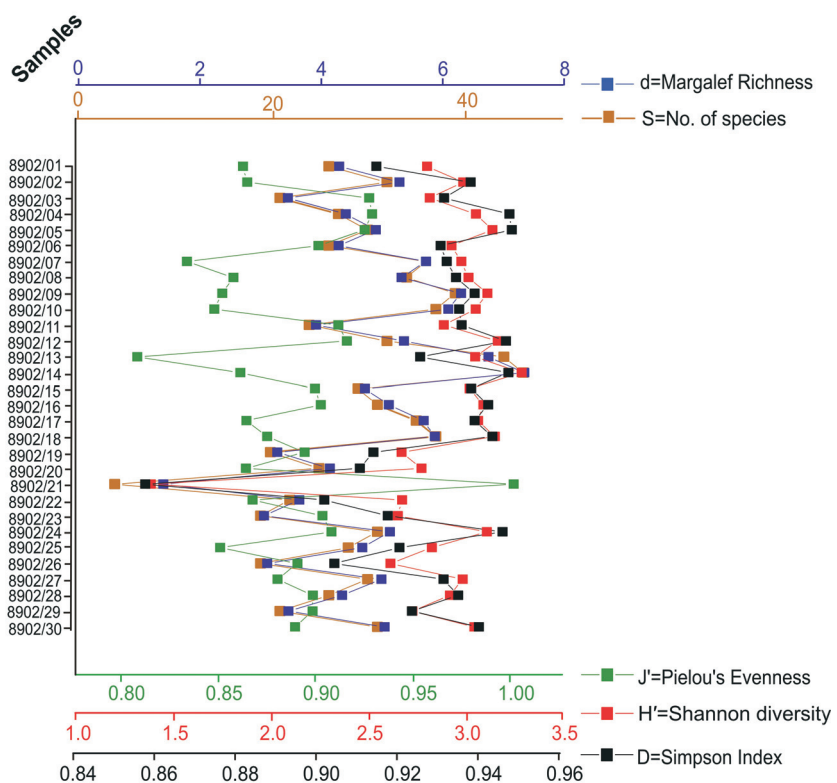
TABLE 4

Ecological preferences of the recovered species of radiolarian taxa from the studied outcrop: Kalapathar Section (KP), South Pont section (SP) and Laccum Point Section (LP) (only the identified radiolarian taxa up to the species level have been taken into consideration).

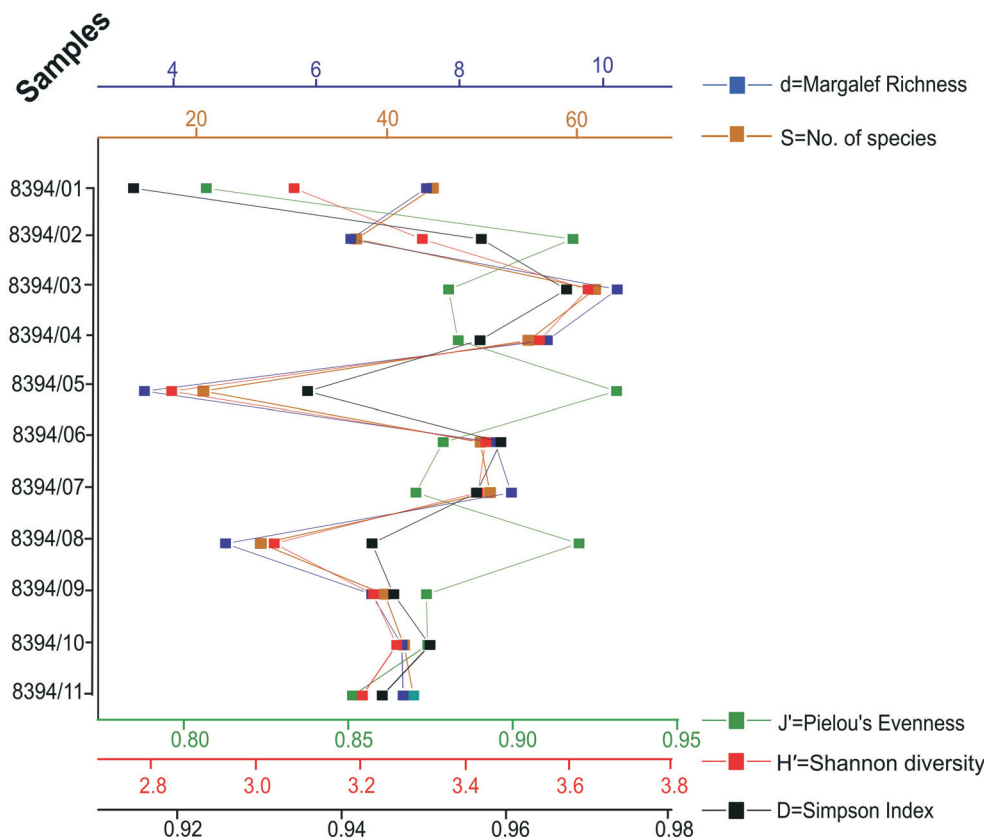
<b>Radiolarian Taxa</b>	<b>Outcrops/Sections</b>	<b>Ecological preferences</b>	<b>Sources &amp; date of citation</b>
<i>Acrobotrys cribosa</i>	KP; SP; LP	Cosmopolitan	<a href="https://www.pangaea.de">https://www.pangaea.de</a> ; 8/1/2021
<i>Acrobotrys isolenia</i>	KP; SP; LP	Warm	<a href="https://www.pangaea.de">https://www.pangaea.de</a> ; 8/1/2021
<i>Acrosphaera spinosa</i>	SP; LP	Cosmopolitan	<a href="https://www.pangaea.de">https://www.pangaea.de</a> ; 30/4/2021
<i>Amphistylus angelinus</i>	KP; SP; LP	Cosmopolitan	<a href="https://www.pangaea.de">https://www.pangaea.de</a> ; 4/1/2021
<i>Artostrobus annulatus</i>	KP; SP; LP	Cosmopolitan	Suzuki (2009)
<i>Botryocyrtis scutum</i>	KP; SP; LP	Warm	Boltovskoy (1998)
<i>Calocycletta costata</i>	KP; SP; LP	Warm tropical to subtropical	<a href="https://www.pangaea.de">https://www.pangaea.de</a> ; 8/1/2021
<i>Calocycletta robusta</i>	KP; SP; LP	Warm tropical to subtropical	<a href="https://www.pangaea.de">https://www.pangaea.de</a> ; 8/1/2021
<i>Carpocanarium papillosum</i>	KP; SP; LP	Cosmopolitan	<a href="https://www.pangaea.de">https://www.pangaea.de</a> ; <a href="https://www.gbif.org">https://www.gbif.org</a> ; 25/12/2020
<i>Carpocanarium kinugasense</i>	KP; SP; LP	Subtropical	<a href="https://www.pangaea.de">https://www.pangaea.de</a> ; 25/12/2020
<i>Carpocanopsis cristatum</i>	KP; SP; LP	Tropical to subtropical	<a href="https://www.pangaea.de">https://www.pangaea.de</a> ; 25/12/2020
<i>Clathrocanium sphaerocephalum</i>	KP; SP; LP	Tropical to subtropical	<a href="https://www.pangaea.de">https://www.pangaea.de</a> ; 25/12/2020
<i>Collosphaera brattstroemi</i>	LP	Cosmopolitan	<a href="https://www.pangaea.de">https://www.pangaea.de</a> ; <a href="https://www.gbif.org">https://www.gbif.org</a> ; 25/12/2020
<i>Collosphaera macropora</i>	SP; LP	Warm	Boltovskoy (1998)
<i>Cornutella profunda</i>	KP; SP; LP	Cosmopolitan	Boltovskoy & Correa (2016)
<i>Cyrtocapsella cornuta</i>	SP; LP	Cosmopolitan	<a href="https://www.pangaea.de">https://www.pangaea.de</a> ; <a href="https://www.gbif.org">https://www.gbif.org</a> ; 25/12/2020
<i>Cyrtocapsella tetraperata</i>	SP; LP	Cosmopolitan	Suzuki (2009)
<i>Dendrospyris bursa</i>	KP; SP; LP	Tropical to subtropical	<a href="https://www.pangaea.de">https://www.pangaea.de</a> ; <a href="https://www.gbif.org">https://www.gbif.org</a> ; 25/12/2020
<i>Dendrospyris pododendros</i>	SP	Tropical to subtropical	<a href="https://www.pangaea.de">https://www.pangaea.de</a> ; <a href="https://www.gbif.org">https://www.gbif.org</a> ; 25/12/2020
<i>Didymocyrtis basanii</i>	SP	Cosmopolitan	<a href="https://www.pangaea.de">https://www.pangaea.de</a> ; 25/12/2020
<i>Didymocyrtis laticonus</i>	SP	Cosmopolitan	pangea and <a href="https://www.gbif.org">https://www.gbif.org</a> ; 25/12/2020
<i>Didymocyrtis mammifera</i>	KP; SP; LP	Tropical to subtropical	<a href="https://www.pangaea.de">https://www.pangaea.de</a> ; 25/12/2020
<i>Didymocyrtis prismatica</i>	KP	Tropical to subtropical	<a href="https://www.pangaea.de">https://www.pangaea.de</a> ; 25/12/2020
<i>Dorcadospyrus alata</i>	SP; LP	Tropical to subtropical	<a href="https://www.pangaea.de">https://www.pangaea.de</a> ; 25/12/2020
<i>Dorcadospyrus dentata</i>	KP	Tropical to subtropical	<a href="https://www.pangaea.de">https://www.pangaea.de</a> ; 25/12/2020
<i>Druppatractus irregularis</i>	KP; SP	Warm	Boltovskoy (1998)
<i>Druppatractus nanus</i>	LP	Cosmopolitan	<a href="https://www.pangaea.de">https://www.pangaea.de</a> ; <a href="https://www.gbif.org">https://www.gbif.org</a> ; 25/12/2020
<i>Euceryphalus histricosus</i>	SP	Cosmopolitan	<a href="https://www.pangaea.de">https://www.pangaea.de</a> ; <a href="https://www.gbif.org">https://www.gbif.org</a> ; 25/12/2020
<i>Eucyrtidium hexagonatum</i>	KP; LP	Cosmopolitan	<a href="https://www.pangaea.de">https://www.pangaea.de</a> ; <a href="https://www.gbif.org">https://www.gbif.org</a> ; 25/12/2020
<i>Giraffospyris toxaria</i>	KP; SP	Warm tropical to subtropical	<a href="https://www.pangaea.de">https://www.pangaea.de</a> ; 25/12/2020
<i>Heliodiscus echiniscus</i>	KP; SP; LP	Warm	<a href="https://www.pangaea.de">https://www.pangaea.de</a> ; 25/12/2020
<i>Hexacontium pachydermum</i>	SP	Cosmopolitan	<a href="https://www.pangaea.de">https://www.pangaea.de</a> and <a href="https://www.gbif.org">https://www.gbif.org</a> ; 26/12/2020
<i>Hexapyle dodecantha</i>	KP; SP	Cosmopolitan	<a href="https://www.pangaea.de">https://www.pangaea.de</a> ; 25/12/2020
<i>Hexastylus dimensivus</i>	SP	Warm	<a href="https://www.pangaea.de">https://www.pangaea.de</a> ; 25/12/2020
<i>Lamprocycles margatenensis</i>	SP; LP	Tropical to subtropical	<a href="https://www.pangaea.de">https://www.pangaea.de</a> ; <a href="https://www.gbif.org">https://www.gbif.org</a> ; 26/12/2020
<i>Larcopyle nebulum</i>	SP; LP	Cosmopolitan	<a href="https://www.pangaea.de">https://www.pangaea.de</a> ; 26/12/2020
<i>Larcopyle pylomaticus</i>	SP; LP	Cosmopolitan	<a href="https://www.pangaea.de">https://www.pangaea.de</a> ; 4/1/2021
<i>Larcospira quadrangula</i>	SP	Warm	Boltovskoy (1998)
<i>Liriospyris elevata</i>	KP; SP; LP	Warm	<a href="https://www.pangaea.de">https://www.pangaea.de</a> ; 4/1/2021
<i>Liriospyris globosa</i>	KP; SP; LP	Warm	<a href="https://www.pangaea.de">https://www.pangaea.de</a> ; 4/1/2021
<i>Liriospyris mutuaria</i>	KP; SP; LP	Warm	<a href="https://www.pangaea.de">https://www.pangaea.de</a> ; 4/1/2021
<i>Liriospyris parkerae</i>	KP; SP; LP	Warm	<a href="https://www.pangaea.de">https://www.pangaea.de</a> ; 4/1/2021
<i>Otosphaera polymorpha</i>	KP; SP; LP	Warm tropical to subtropical	<a href="https://www.pangaea.de">https://www.pangaea.de</a> ; 27/12/2020
<i>Peripherina decora</i>	SP	Cosmopolitan	<a href="https://www.pangaea.de">https://www.pangaea.de</a> ; <a href="https://www.gbif.org">https://www.gbif.org</a> ; 4/1/2021
<i>Phormostichoartus dolodium</i>	KP; SP; LP	Tropical to subtropical	<a href="https://www.pangaea.de">https://www.pangaea.de</a> ; 27/12/2020
<i>Phormostichoartus marylandicus</i>	KP; SP; LP	Cosmopolitan	<a href="https://www.pangaea.de">https://www.pangaea.de</a> ; <a href="https://www.gbif.org">https://www.gbif.org</a> ; 28/12/2020
<i>Lithopera thornburgi</i>	LP	Tropical to subtropical	<a href="https://www.pangaea.de">https://www.pangaea.de</a> ; <a href="https://www.gbif.org">https://www.gbif.org</a> ; 27/12/2020
<i>Siphocampe arachnea</i>	SP; LP	Cosmopolitan	Lazarus et al. (2006)
<i>Siphocampe lineata</i>	KP; SP; LP	Cosmopolitan	Suzuki (2009); Lazarus et al. (2006); <a href="https://www.pangaea.de">https://www.pangaea.de</a> ; <a href="https://www.gbif.org">https://www.gbif.org</a> ; 28/12/2020
<i>Siphostichoartus corona</i>	SP; LP	Tropical to subtropical	<a href="https://www.pangaea.de">https://www.pangaea.de</a> ; 27/12/2020
<i>Solenosphaera zanguebarica</i>	KP	Tropical to sub tropical	<a href="https://www.pangaea.de">https://www.pangaea.de</a> ; 27/12/2020
<i>Sphaerostylus cristatus</i>	KP	Cosmopolitan	<a href="https://www.pangaea.de">https://www.pangaea.de</a> ; 4/1/2021
<i>Spongocore puella</i>	LP	Cosmopolitan	<a href="https://www.pangaea.de">https://www.pangaea.de</a> ; <a href="https://www.gbif.org">https://www.gbif.org</a> ; 30/12/2020
<i>Stichocorys delmontensis</i>	KP; SP; LP	Cosmopolitan	<a href="https://www.pangaea.de">https://www.pangaea.de</a> ; <a href="https://www.gbif.org">https://www.gbif.org</a> ; 30/12/2020
<i>Stylatracus sanctaeannae</i>	KP; SP; LP	Cosmopolitan	<a href="https://www.pangaea.de">https://www.pangaea.de</a> ; 4/1/2021
<i>Stylatracus universus</i>	KP; SP; LP	Cosmopolitan	<a href="https://www.pangaea.de">https://www.pangaea.de</a> ; 4/1/2021
<i>Stylocidictya temuispina</i>	KP; SP; LP	Warm tropical to subtropical	<a href="https://www.pangaea.de">https://www.pangaea.de</a> ; 30/12/2020
<i>Stylocidictya validispina</i>	KP; SP; LP	Cosmopolitan	<a href="https://www.pangaea.de">https://www.pangaea.de</a> ; <a href="https://www.gbif.org">https://www.gbif.org</a> ; 1/1/2021
<i>Stylosphaera radiosa</i>	LP	Cosmopolitan	<a href="https://www.pangaea.de">https://www.pangaea.de</a> ; <a href="https://www.gbif.org">https://www.gbif.org</a> ; 1/1/2021
<i>Tetrapyle octacantha</i>	KP; SP; LP	Cosmopolitan	<a href="https://www.pangaea.de">https://www.pangaea.de</a> ; 30/4/2021
<i>Tymanidium binoculum</i>	KP; SP; LP	Warm	<a href="https://www.pangaea.de">https://www.pangaea.de</a> ; <a href="https://www.gbif.org">https://www.gbif.org</a> ; 4/1/2021



TEXT-FIGURE 4A  
Diversity indices of radiolarian taxa from the Kalapathar Section.



TEXT-FIGURE 4B  
Diversity indices of radiolarian taxa from the South Point Section.



TEXT-FIGURE 4C  
Diversity indices of radiolarian taxa from the Laccam Point Section.

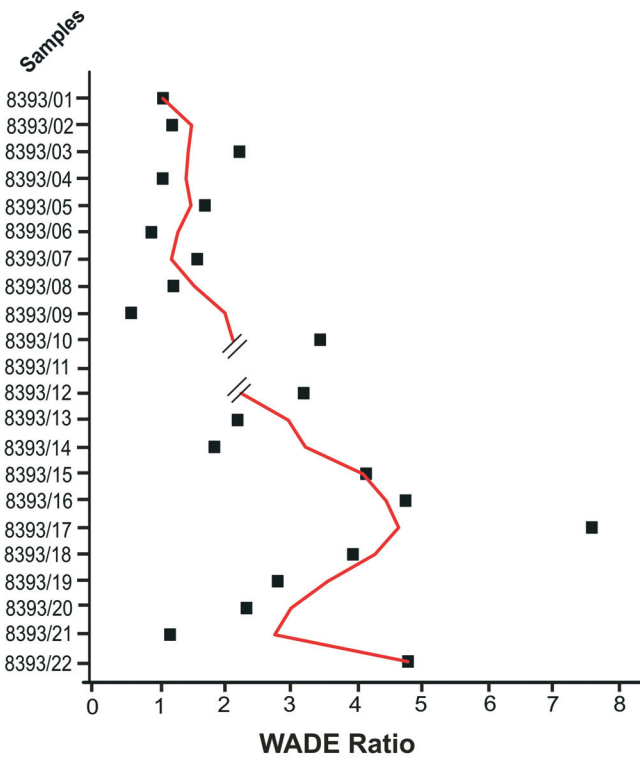
DSDP Leg 24 (site 238) drilled at West-Central Indian Ocean and Gulf of Aden (Sanfilippo and Riedel 1974), ODP Leg 115 (Site 709) drilled at the western part of the Indian Ocean (Johnson 1990), ODP Leg 116 (sites 717-719) drilled at the Bengal fan, eastern part of the Indian Ocean (Takahashi 1990), IODP Expedition 359 (sites U1466 and U1467) drilled at the Maldives (Betzler et al. 2017). From sites 213 and 214 of DSDP Leg 22, *Dorcadospyris alata* Zone, and from Site 216 of DSDP Leg 22, both *Calocycletta costata* and *Dorcadospyris alata* zones have been identified by Johnson (1974). Sanfilippo and Riedel (1974) also reported *Dorcadospyris alata* and *Calocycletta costata* zones from DSDP Leg 24 (Site 238). In the rest of the DSDP, ODP, and IODP sites radiolarians have been reported, however, no radiolarian zones have been assigned.

The present radiolarian assemblages are also comparable to those of Mahapatra and Sharma (1994), Sharma and Daneshian (1998, 2003), Sharma et al. (1999), Sharma and Ram (2003), and Sharma et al. (2007, 2011) reported from the onshore sections of isolated islands of the Andaman-Nicobar Basin where both the *Calocycletta costata* and *Dorcadospyris alata* zones have been identified (Table 6). The *Calocycletta costata* Zone has been delineated from the Colebrook, North Passage and Great Nicobar Islands (Mahapatra and Sharma 1994; Sharma and Ram 2003; Sharma et al. 2011), Nicholson Island (Sharma and Daneshian 1998; 2003), John Lawrence Island (Sharma and Daneshian 1998), Strait, Nicholson, Havelock and Henry Lawrence islands (Sharma and Ram 2003), Inglis Island (Sharma et

al. 2007). On the other hand, the *Dorcadospyris alata* Zone has been demarcated from Nicholson Island (Sharma and Daneshian 1998), Colebrook, North Passage, and Great Nicobar islands (Sharma and Ram 2003; Sharma et al. 2011), Nancowry and Kamorta islands (Sharma et al. 1999; Sharma and Daneshian 2003).

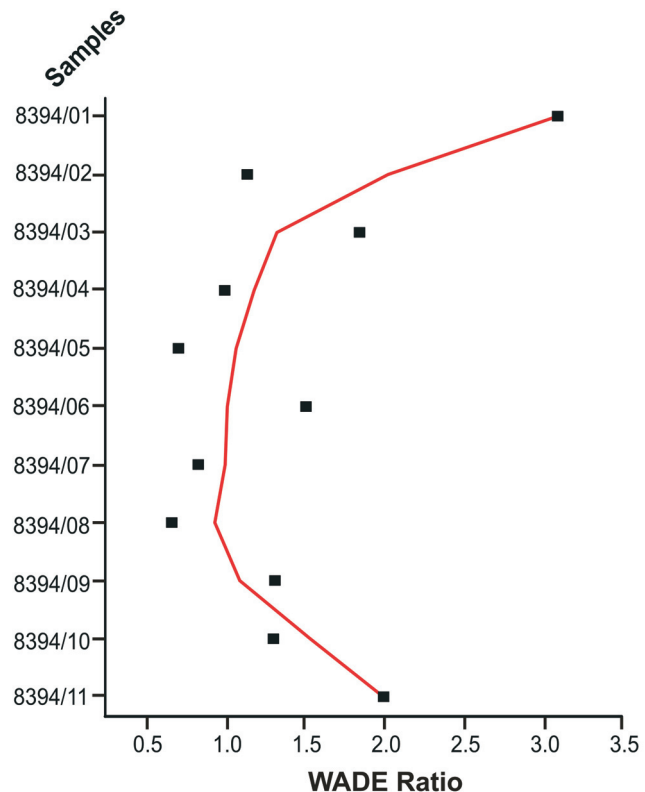
#### Paleoecology

For paleoecological analysis, the WADE index is a very useful tool, which is deduced from the ratios of deep-dwelling and surface species of radiolarians (Lazarus et al. 2006). Eventually, the WADE index is considered to be a good indicator of productivity (Lazarus 2005; Lazarus et al. 2006). The ecological data, based on living forms, can efficiently be used for the late Miocene, and also can be extended into older time intervals to interpret ecology based on paleobiogeographic distributions (Lazarus 2005). However, there are certain limitations because it is very difficult to decipher the exact bathymetry based on radiolarian species both in the modern ocean as well as in older sediments (Lazarus 2005). The data source for the ecological preferences of the radiolarian species, recorded herein, has already been mentioned in the material and methods section, and is presented in Table 4. The result of the present study indicates that the Burdigalian-Langhian radiolarians from the Kalapathar and South Point sections and Langhian-Serravallian radiolarians of the Laccam Point Section are dominated by warm-water species. However, in the Kalapathar Section warm-water species are more preponderant (text-fig. 5A) as denoted by higher



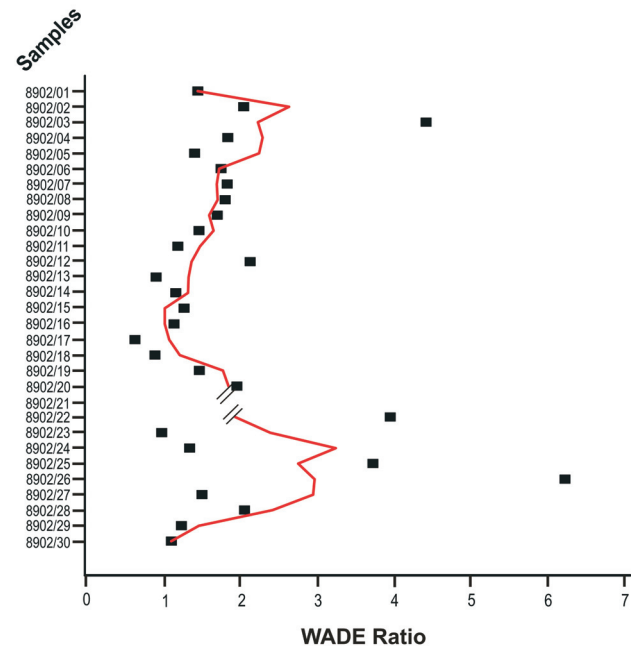
TEXT-FIGURE 5A

Graphical representations of WADE ratio with respect to samples from the Kalapathar Section.



TEXT-FIGURE 5C

Graphical representations of WADE ratio with respect to samples from the Laccam Point Section.



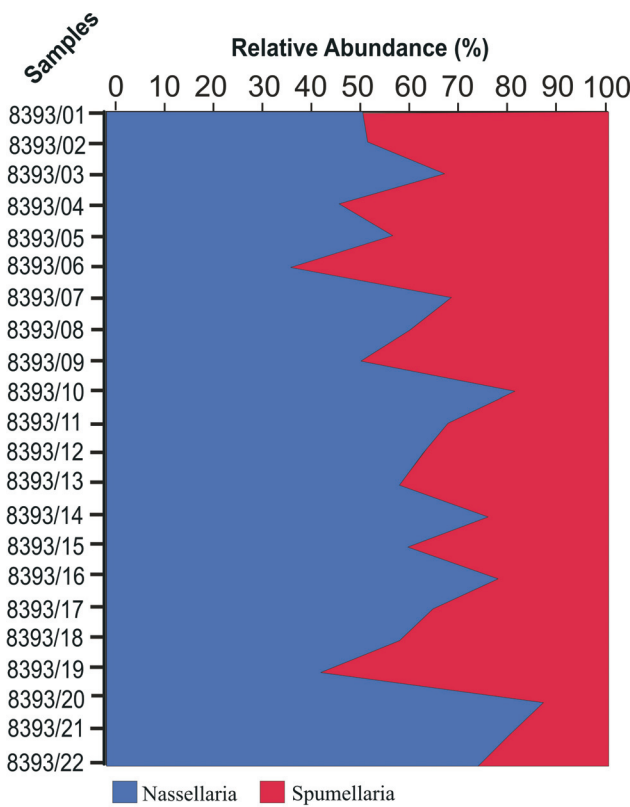
TEXT-FIGURE 5B

Graphical representations of WADE ratio with respect to samples from the South Point Section.

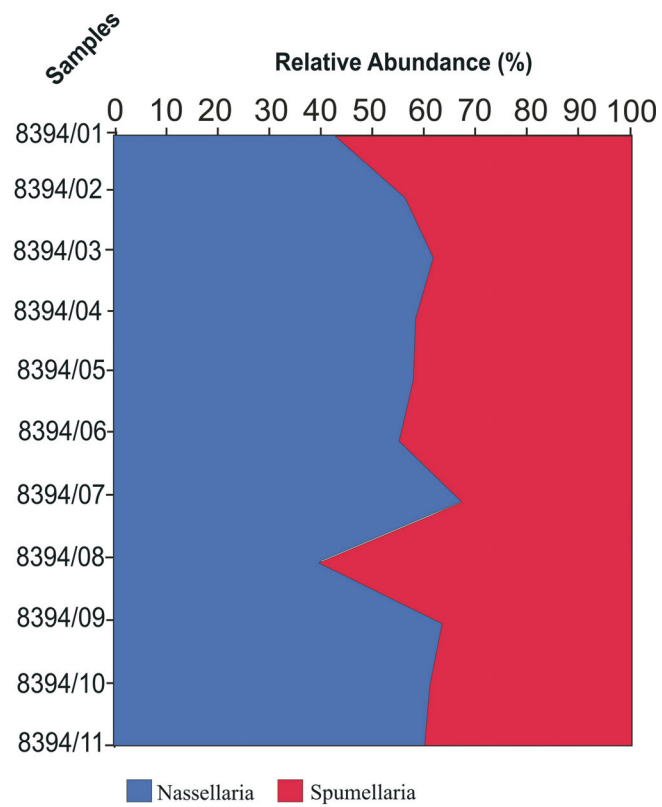
positive ratios in comparison to the other two sections. Overall, in all three sections, the WADE ratio shows corresponding shift towards higher values that implies lower export productivity during Burdigalian-Langhian time.

Böhme (2003) suggested that the warm period during the middle Miocene ended abruptly between 14.0–13.5 Ma. It has been documented from the southeast Indian Ocean that during the late early to early middle Miocene the diversity of the benthic foraminifera increased along with low  $\delta^{18}\text{O}$  and high  $\delta^{13}\text{C}$  values that envisage warm bottom water with low nutrient supply (Rai and Maurya 2009). Using clumped isotope and Mg/Ca ratio from the Indian Ocean, Modestou et al. (2020) estimated the rise in temperature to  $11.0 \pm 1.7^\circ\text{C}$  (between 15 and 17 Ma) during the middle Miocene Climatic Optimum (MCO, 14.7–17 Ma) and  $8.1 \pm 1.9^\circ\text{C}$  (between 11.5 and 13 Ma) after the transition of middle Miocene Climate, i.e., 13.0–14.7 Ma. Their study indicates that during that time the temperature was about 6 to  $9^\circ\text{C}$  warmer than the present. In a previous study carried out from the Kalapathar Section of Havelock Island, Chakraborty et al. (2019) reported possible MCO event based on multiple microfossils. The present study also confirms that during the late early to early middle Miocene warm-water radiolarians were overwhelmingly dominant that may be correlated to the MCO event.

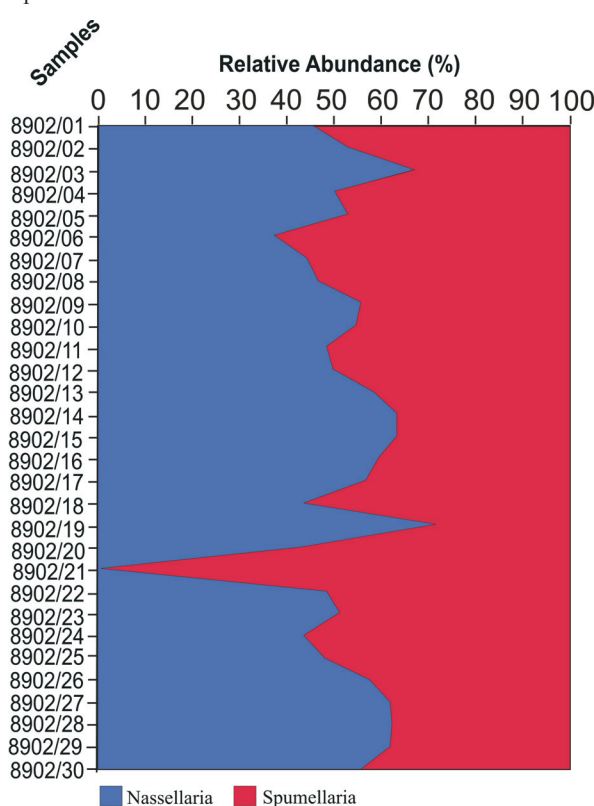
The four radiolarian species reported herein for the first time from the northeastern part of the Indian Ocean are *Eucecrys-*



TEXT-FIGURE 6A  
Nassellaria-Spumellaria ratio with respect to samples from the Kalapathar Section.



TEXT-FIGURE 6C  
Nassellaria-Spumellaria ratio with respect to samples from the Laccam Point Section.



TEXT-FIGURE 6B  
Nassellaria-Spumellaria ratio with respect to samples from the South Point Section.

*phalus histricosus*, *Hexacontium pachydermum*, *Larcopyle pylomaticus* and *Stylodictya tenuispina*. Most of the species are stratigraphically long ranging and are common in the Miocene. In the present-day ocean as well as in fossil record the cosmopolitan species *Eucecrysphalus histricosus* is geographically distributed in the Pacific Ocean (Ling et al. 2005; Welling 2003), Peru margin (de Wever et al. 1990), Namibia (Jacot des Combes and Abelmann 2007) and Arctic Ocean (Schröder-Ritzrau 2001). As evident from the published literature, in the fossil record as well as in modern oceans *Hexacontium pachydermum* is distributed in the Pacific Ocean (Kamikuri et al. 2009b), Atlantic Ocean (Labracherie et al. 2005), and some parts of Norway (Jørgensen 1905). *Larcopyle pylomaticus* is also a cosmopolitan species and has been recorded both as fossils and recent radiolarian assemblages from the Pacific Ocean (Hernández-Almeida et al. 2020) and the Southern Ocean (Lazarus et al. 2005). *Larcopyle pylomaticus* also has been reported from the middle Miocene to late Pleistocene of Japan Sea by Kamikuri et al. (2017). The distribution of *Stylodictya tenuispina* is known both as a fossil as well as in the present-day Pacific Ocean (Levykina 1986) and Atlantic Ocean (Labracherie et al. 2005).

#### Diversity

Present-day radiolarians are most abundant at or near the equator (Boltovskoy and Jankilevich 1985 and references therein) and it has been confirmed that in comparison to subequatorial region, zooplankton abundances at the equator, specifically radiolarian assemblages are more pronounced (Boltovskoy and Jankilevich 1985).

TABLE 5

Comparison of the common radiolarian taxa recorded in the studied samples from Havelock Island with other known late early to early middle Miocene assemblages recorded from nearby sites of DSDP, ODP and IODP Expeditions (P=Present study).

Common Radiolarian Taxa	DSDP				ODP Sites		IODP Betzler et al. (2017), 359 Sites U1466 and U1467, Maldives
	Johnson (1974), Leg 22 Sites 211, 213, 214 and 216, eastern Indian Ocean		Sanfilippo and Riedel (1974), Leg 24, Site 238, West-Central Indian Ocean and Gulf of Aden		Takahashi (1990), Leg 116 Sites 717-719, Bengal fan, eastern Indian Ocean	Johnson (1990), Leg 115, Site 709, western Indian Ocean	
	211	213	214	216			
<i>Acrosphera spinosa</i>					P		
<i>Artostrobus annulatus</i>					P		
<i>Calocycletta costata</i>		P		P			
<i>Carpocanarium papillosum</i>					P		
<i>Collosphaera macropora</i>					P		
<i>Carpocanopsis cristatum</i>		P					
<i>Cornutella profunda</i>					P		
<i>Cyrtocapsella cornuta</i>	P			P			
<i>Cyrtocapsella tetraptera</i>				P			
<i>Dendrospyris bursa</i>				P		P	
<i>Didymocyrtis laticonus</i>					P		
<i>Dorcadospyris alata</i>	P	P	P	P			
<i>Dorcadospyris dentata</i>		P		P			
<i>Otosphaera polymorpha</i>					P		
<i>Phormostichoartus doliodum</i>						P	
<i>Siphostichartus corona</i>					P	P	
<i>Siphocampe arachnea</i>					P		
<i>Siphocampe lineata</i>					P		
<i>Stichocorys delmontensis</i>	P	P	P	P	P	P	
<i>Stylatractus universes</i>						P	
<i>Tetrapyle octacantha</i>					P		P

As revealed from the present analysis, in all three studied sections both Nassellaria and Spumellaria are abundant, however, the forms belonging to Nassellaria are marginally dominant in some instances (Tables 1-3; text-figs. 6A-C). Some evidence supports that the forms of Nassellaria inhabited in deeper waters in comparison to Spumellaria (Boltovskoy and Jankilevich 1985 and references therein). The marginal dominance of Nassellaria in some instances indicates that the deposition took place in a slightly deep-water setting to marginal sea. Although radiolaria can live in water depth of thousands of meters in the sea, most of them dwell in the upper water layer, and it is less likely that slightly deep water could result in the increase in the abundance of nassellarians. In general, the species dwelling in deeper water feed mainly on detritus and bacterivore (Casey et al. 1979; Anderson et al. 1989; Nimmergut and Abelmann 2002), and their production are more likely controlled by the

export productivity in the upper water layer. Therefore, the marginal dominance of Nassellaria in some instances in this study might have been related to minor changes in export productivity in the surface water.

The overall Shannon diversity index of the three outcrops (text-figs. 4A-C) indicates that the diversity of radiolarians was high during Burdigalian-Langhian, which is dominated by warm species. In some instances, in the Kalapathar and South Point sections, the diversity is the lowest and that is reflected in the graph plotted for the WADE ratio (text-figs. 5A-C). However, in the Laccam Point Section it has been noticed that the sample, which has the lowest diversity, shows a lower WADE ratio (where the warm species are low in comparison to cosmopolitan).

TABLE 6

Comparison of the common radiolarian taxa recorded in the studied samples from Havelock Island with other known late early to early middle Miocene assemblages reported from onshore sections of different islands of the Andaman-Nicobar Basin (P=Present study).

Common Radiolarian Taxa	Radiolarians reported from onshore sections of different islands of the Andaman–Nicobar Basin						
	Mahapatra and Sharma (1994)	Sharma and Daneshian (1998)	Sharma et al. (1999)	Sharma and Daneshian (2003)	Sharma and Ram (2003)	Sharma et al. (2007)	Sharma et al. (2011)
<i>Actinomma</i> sp.	P						
<i>Amphistylus</i> sp.	P						
<i>Calocycletta costata</i>	P	P	P	P	P	P	P
<i>Carpocanarium</i> sp.	P	P	P	P	P	P	
<i>Carpocanistrum</i> spp.	P	P	P	P	P	P	
<i>Circodiscus</i> spp.	P		P	P			
<i>Clathrocanium sphaerocephalum</i>			P				
<i>Collosphaera</i> sp.	P				P		
<i>Collosphaera macropora</i>			P				
<i>Carpocanopsis cristatum</i>	P				P		
<i>Clathrocanium sphaerocephalum</i>	P				P		
<i>Cornutella profunda</i>	P	P			P		
<i>Cyrtocapsella cornuta</i>	P	P			P		
<i>Cyrtocapsella tetrapera</i>	P	P			P		
<i>Dendrospyris bursa</i>	P	P	P	P	P		
<i>Didymocystis laticonus</i>		P	P	P			
<i>Didymocystis prismatica</i>	P				P	P	
<i>Didymocystis mammifera</i>	P			P	P	P	
<i>Dorcadospyrus alata</i>	P		P	P			
<i>Dorcadospyrus dentata</i>	P	P			P	P	
<i>Druppatractus</i> sp.					P		
<i>Druppatractus irregularis</i>	P		P		P		
<i>Druppatractus nanus</i>	P		P		P	P	
<i>Eucyrtidium hexagonatum</i>	P		P	P	P	P	
<i>Giraffospyrus toxaria</i>	P	P	P		P	P	P
<i>Heliodiscus echiniscus</i>					P		
<i>Hexapyle</i> sp.	P						
<i>Liriospyris elevata</i>	P	P	P		P	P	
<i>Liriospyris globosa</i>	P	P			P	P	
<i>Liriospyris mutuaria</i>	P	P	P	P	P	P	
<i>Liriospyris parkerae</i>	P	P	P				P
<i>Liriospyris</i> spp.	P			P	P		
<i>Lithopera thomburgi</i>			P				
<i>Peridium</i> sp.				P		P	
<i>Phormostichoartus marylandicus</i>	P	P	P		P	P	
<i>Siphostichartus corona</i>	P	P			P	P	
<i>Siphocampe arachnea</i>	P				P		
<i>Siphocampe lineata</i>	P				P		
<i>Sphaerostylus cristatus</i>	P				P		
<i>Spongodiscus</i> spp.	P			P	P	P	P
<i>Stictocorys delmontensis</i>	P	P	P		P	P	P
<i>Stylatractus universes</i>					P		
<i>Stylatractus</i> sp.	P				P		
<i>Stylocytya validispina</i>	P	P			P		
<i>Tetrapyle octacantha</i>	P			P	P	P	
<i>Tympnomma binoculum</i>	P	P				P	
<i>Tholospyris</i> sp.	P						

## CONCLUSIONS

One hundred nineteen taxa belonging to 70 genera have been identified from a comprehensive analysis on the radiolarians from the outcrops of Havelock Island; out of which four species namely, *Eucecryphalus histricosus*, *Hexacontium pachydermum*, *Larcopyle pylomaticus*, and *Stylocycta tenuispina* have been recorded for the first time from the northeastern part of the Indian Ocean. The study undertaken on the three outcrops of Havelock Island in the Andaman-Nicobar Basin enumerates the RN4 and RN5 zones based on the index radiolarian species *C. costata* and *D. alata*. A Burdigalian-Langhian age has been assigned for the Kalapathar and South Point sections, however, for the Laccam Point Section a Langhian-Serravallian age has been proposed due to the presence of *L. thornburgi*. The cumulative relative age has been estimated as <17.03 Ma to 13.60/13.63 Ma for the three sections based on the FO and LO of the index radiolarian species. The diversity analysis indicates that the overall diversity of radiolarians was high, and the Nassellaria-Spumellaria ratio indicates that the deposition took place in to some extent a deep-water setting to marginal sea. The WADE ratio suggests a corresponding shift towards higher values that implies lower export productivity. Substantial domi-

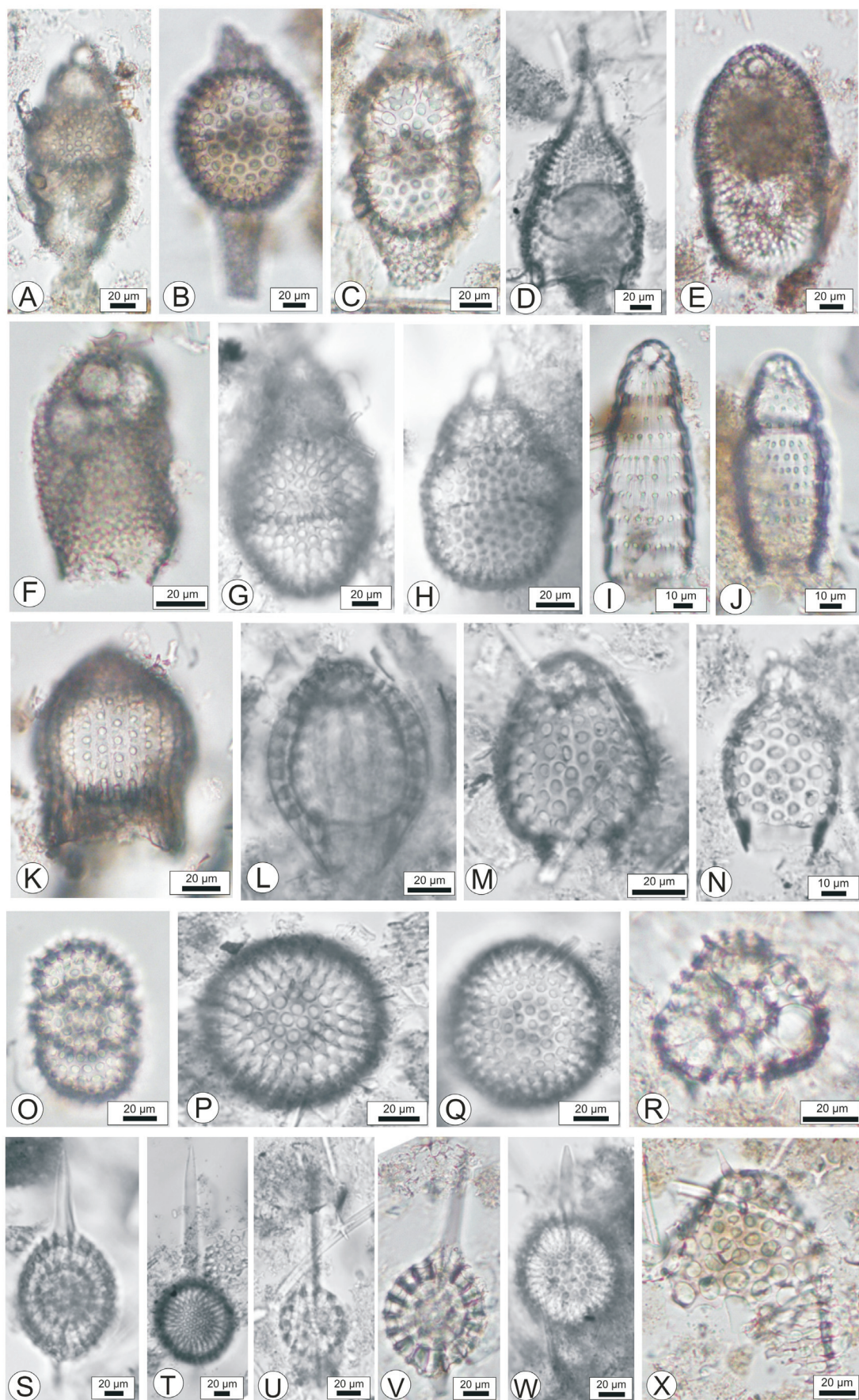
nance of warm-water species of radiolarians during <17.03 Ma to 13.60/13.63 Ma indicates that the possible effect of the MCO event continued till 13.60/13.63 Ma.

## ACKNOWLEDGMENTS

We are thankful to Dr. Vandana Prasad, Director, Birbal Sahni Institute of Palaeosciences, Lucknow, India for her kind permission (BSIP/RDCC/Publication No.16/2021-22) to carry out this work and for providing essential laboratory facilities. We are also grateful to Dr. David Lazarus (Museum für Naturkunde, Humboldt University Berlin, Germany) for his help in reconfirming the identification of radiolarians. Sincere thanks are due to Prof. Micheal A. Kaminski the chief editor, and to Prof. Galina Nestell, associate editor of Micropaleontology, for their valuable suggestions and useful comments. We thank Dr. Qiang Zhang of South China Sea Institute of Oceanology (Chinese Academy of Sciences), China for critically reviewing the manuscript that substantially improved the quality of the manuscript. R.D. is thankful to Department of Science and Technology, Government of India for the award of DST-INSPIRE Fellowship (IF 170761). A. K. B. is thankful to the Head, Department of Applied Geology, IIT (ISM), Dhanbad. A. C. is thankful to

## PLATE 1

- A *Stichocorys delmontensis* (BSIP Slide No. 16834; Sample No. 8394/06),
- B *Didymocyrtis prismatica* (BSIP No. 16831; Sample No. 8393/20),
- C *Didymocyrtis mammifera* (BSIP Slide No. 16859; Sample No. 8902/01),
- D *Lamprocyclas margatensis* (BSIP Slide No. 16856; Sample No. 8902/19),
- E *Lithopera thornburgi* (BSIP Slide No. 16837; Sample No. 8394/11),
- F *Botryocyrtis scutum* (BSIP Slide No. 16832; Sample No. 8393/15),
- G *Cyrtocapsella cornuta* (BSIP Slide No. 16836; Sample No. 8394/05),
- H *Cyrtocapsella tetrapera* (BSIP Slide No. 16858; Sample No. 8902/04),
- I *Siphocampe arachnea* (BSIP Slide No. 16848; Sample No. 8902/14),
- J *Sipocamphe lineata* (BSIP Slide No. 16857; Sample No. 8902/11),
- K *Carpocanopsis cristata* (BSIP Slide No. 16834; Sample No. 8394/06),
- L *Carpocanium kinugasense* (BSIP Slide No. 16830; Sample No. 8393/18),
- M *Carpocanarium aff. papillosum* (BSIP Slide No. 16854; Sample No. 8902/22),
- N *Carpocanarium papillosum* (BSIP Slide No. 16855; Sample No. 8902/22),
- O *Tholonid* sp. (BSIP Slide No. 16850; Sample No. 8902/13),
- P *Actinomma medusa?* (BSIP Slide No. 16844; Sample No. 8902/20),
- Q *Carposphaera* sp. (BSIP Slide No. 16854; Sample No. 8902/22),
- R *Hexapyle dodecantha* (BSIP Slide No. 16828; Sample No. 8393/22),
- S *Stylatractus santaeannae* (BSIP Slide No. 16848; Sample No. 8902/14),
- T *Stylatractus universes* (BSIP Slide No. 16842; Sample No. 8902/23),
- U *Druppatractus irregularis* (BSIP Slide No. 16852; Sample No. 8902/03),
- V *Stylosphaera radios* (BSIP Slide No. 16838; Sample No. 8394/07),
- W *Amphistylus angelinus* (BSIP Slide No. 16847; Sample No. 8902/15),
- X *Eucecryphalus histricosus* (BSIP Slide No. 16848; Sample No. 8902/14).



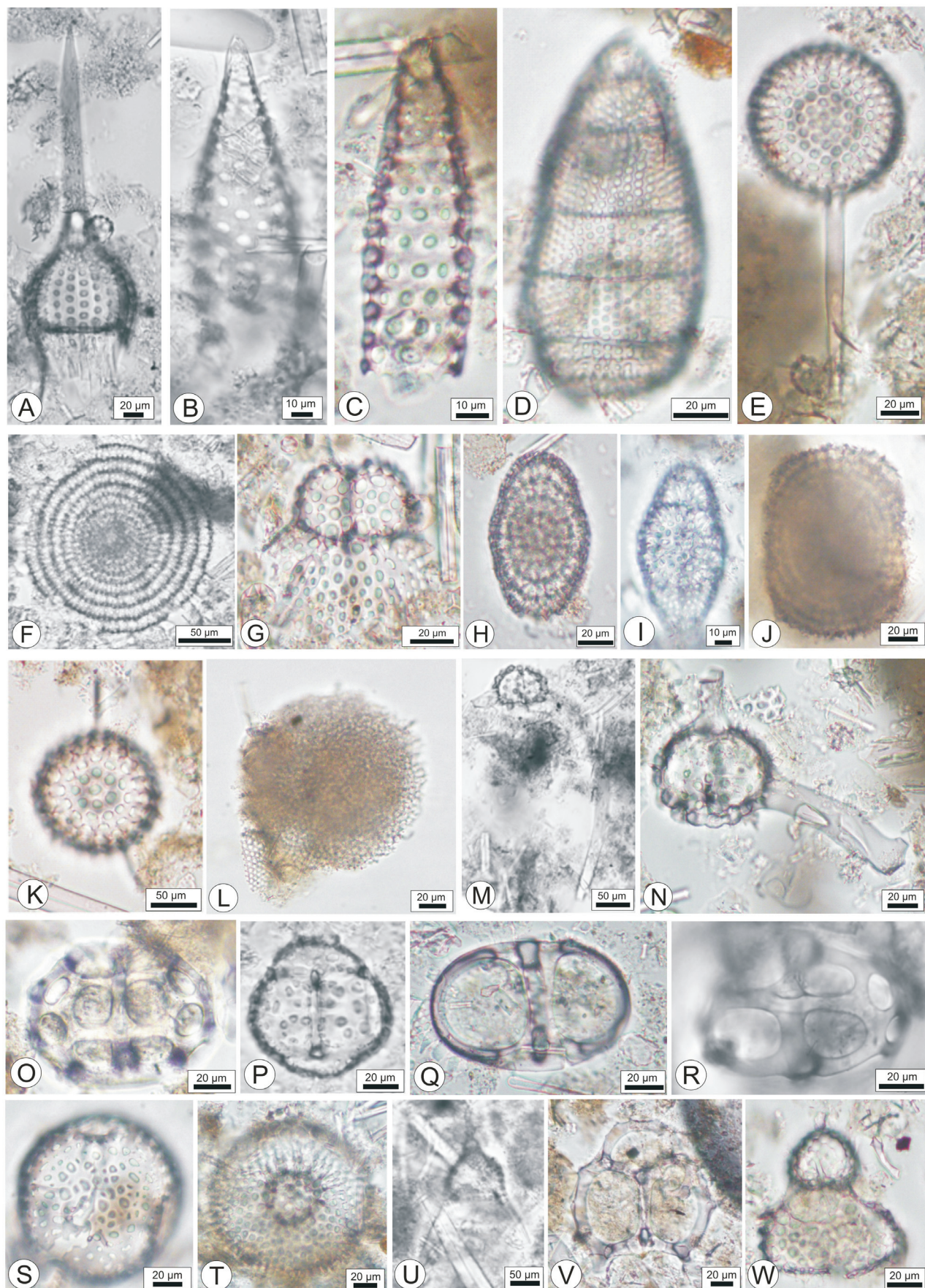
the authorities of BSIP for the fellowship of Birbal Sahni Research Associate (BSRA). L. R. (IF 180259) and S. S. (IF 170181) are also indebted to the Department of Science and Technology, Government of India for the award of DST-IN-SPIRE Fellowship.

## REFERENCES

- ANDERSON, O. R., BENNETT, P., ANGEL, D. and BRYAN, M., 1989. Experimental and observational studies of radiolarian physiological ecology: 2. Trophic activity 119 and symbiont primary productivity of Spongaster tetras tetras with comparative data on predatory activity of some Nassellarida. *Marine Micropaleontology*, 14: 267–273.
- ARMSTRONG, H. A. and BRASIER M. D., 2005. *Microfossils. 2<sup>nd</sup> edition*. Oxford (USA): Blackwell Publishing, 1–287 pp.
- BANDOPADHYAY, P. C. and CARTER, A., 2017. The archipelago group: current understanding. In: Bandopadhyay P.C. and Carter, A., Eds., *The Andaman-Nicobar Accretionary Ridge: Geology, Tectonics and Hazards*. Memoirs 47, 153–166, London: Geological Society.
- BETZLER, C., EBERLI, G. P., ALVAREZ ZARIKIAN, C. A. and THE EXPEDITION 359 SCIENTISTS, 2017. Maldives Monsoon and Sea Level. *Proceedings of the International Ocean Discovery Program 359*. College Station, TX: Ocean Drilling Program. doi: 10.14379/iodp.proc.359.2017.
- BLOIS, J. L. and HADLY, E. A., 2009. Mammalian response to Cenozoic climatic change. *Annual Review of Earth and Planetary Sciences*, 37: 181–208.
- BÖHME, M., 2003. The Miocene climatic optimum: evidence from ectothermic vertebrates of Central Europe. *Palaeogeography, Palaeoclimatology, Palaeoecology*, 195 (3–4): 389–401.
- BOLTOVSKOY, D., 1998. Classification and distribution of South Atlantic Recent polycystine Radiolaria. *Paleontologica Electronica*, 1 (2): 116.
- BOLTOVSKOY, D. and CORREA, N., 2016. Biogeography of Radiolaria Polycystina (Protista) in the World Ocean, *Progress in Oceanography*. doi: 10.1016/j.pocean.2016.09.006
- BOLTOVSKOY, D. and JANKILEVICH, S. S., 1985. Radiolarian distribution in east equatorial Pacific plankton. *Oceanologica Acta*, 8 (1): 101–123.
- CASEY, R., GUST, L., LEAVESLEY, A., WILLIAMS, D., REYNOLDS, R., DUIS, T. and SPAW, M., 1979. Ecological niches

## PLATE 2

- A *Calocyctella costata* (BSIP Slide No. 16827; Sample No. 8393/22),
- B *Cornutella profunda* (BSIP Slide No. 16833; Sample No. 8394/08 ),
- C *Artostrobus annulatus* (BSIP Slide No. 16848; Sample No. 8902/14),
- D *Eucyrtidium hexagonatum* (BSIP Slide No. 16834; Sample No. 8394/06),
- E *Amphisphaera* sp. (BSIP Slide No. 16833; Sample No. 8394/08),
- F *Stylodictya tenuispina* (BSIP Slide No. 16844; Sample No. 8902/20),
- G *Dendrospyris bursa* (BSIP Slide No. 16853; Sample No. 8902/25 ),
- H *Larcopyle polyacantha?* (BSIP Slide No. 16840; Sample No. 8902/24),
- I *Larcopyle nebulum* (BSIP Slide No. 16840; Sample No. 8902/24),
- J *Larcopyle pylomaticus* (BSIP Slide No. 16850; Sample No. 8902/13),
- K *Hexacontium pachydermum* (BSIP Slide No. 16839; Sample No. 8902/27),
- L *Spongodiscus* sp. (BSIP Slide No. 16847; Sample No. 8902/15),
- M *Dorcadospyris alata* (BSIP No. 16841; Sample No. 8902/23),
- N *Dorcadospyris dentata* (BSIP Slide No. 16829; Sample No. 8393/16),
- O *Typanomma binoculum* (BSIP Slide No. 16851; Sample No. 8902/07),
- P *Liriospyris* sp. cf *ovalis* (BSIP Slide No. 16846; Sample No. 8902/16),
- Q *Liriospyris parkerae* (BSIP Slide No. 16852; Sample No. 8902/03),
- R *Liriospyris elevata* (BSIP Slide No. 16849; Sample No. 8902/17),
- S *Collosphaera brattstroemi* (BSIP Slide No. 16835; Sample No. 8394/01),
- T *Heliodiscus echiniscus* (BSIP Slide No. 16840; Sample No. 8902/24),
- U *Lychnocanium audax?* (BSIP Slide No. 16843; Sample No. 8902/21),
- V *Giraffospyris toxaria* (BSIP Slide No. 16845; Sample No. 8902/18),
- W *Clathrocanium sphaerocephalum* (BSIP Slide No. 16836; Sample No. 8394/05).



- of radiolarians, planktonic foraminiferans and pteropods inferred from studies on living forms in the Gulf of Mexico and adjacent waters. *Transactions—Gulf Coast Association of Geological Societies*, 24: 216–223.
- CASEY, R. E., WEINHEIMER, A. L. and NELSON, C. O., 1990. Cenozoic radiolarian evolution and zoogeography of the Pacific. *Bulletin of Marine Science*, 47 (1): 221–232.
- CHAKRABORTY, P. P. and PAL, T., 2001. Anatomy of a forearc submarine fan: Upper Eocene Oligocene Andaman Flysch Group, Andaman Islands, India. *Gondwana Research*, 4: 477–486.
- CHAKRABORTY, A., GHOSH, A. K., DEY, R., SAXENA, S. and MAZUMDER, A., 2019. Record of the Miocene Climate Optimum in the northeast Indian Ocean: evidence from the microfossils. *Palaeobiodiversity and Palaeoenvironments*, 99 (2): 159–175.
- CHAKRABORTY, A., GHOSH, A. K. and SAXENA, S., 2021. Neogene calcareous nannofossil biostratigraphy from northern Indian Ocean: Implications on palaeoceanography and palaeoecology. *Palaeogeography, Palaeoclimatology, Palaeoecology*. doi: doi.org/10.1016/j.palaeo.2021.110583.
- CHEN, M. H., WANG, R. J., YANG, L. H., HAN, J. X. and LU, J. 2003. Development of east Asian summer monsoon environments in the late Miocene: radiolarian evidence from Site 1143 of ODP Leg 184. *Marine Geology*, 201: 169–177.
- CLARKE, K. and GORLEY, R., 2001. Primer E-v5: User Manual/Tutorial, Primer-E. Plymouth 1–91.
- CLEMENS, S. C., KUHNT, W., LEVAY, L. J. and THE EXPEDITION 353 SCIENTISTS, 2016. Indian Monsoon Rainfall, *Proceedings of the International Ocean Discovery Program, 353*. College Station, TX: International Ocean Discovery Program. doi: 10.14379/?iodp.proc.353.2016.
- DE WEVER, P., CAULET, J. P. and BOURGOIS, J., 1990. Radiolarian biostratigraphy from Leg 112 on the Peru Margin. *Proceedings of the Ocean Drilling Program, Scientific Results*, 112: 181–207.
- FIGUEIRIDO, B., JANIS, C. M., PEREZ-CLAROS, J. A., DE RENZI, M. and PALMQVIST, P. 2012. Cenozoic climate change influences mammalian evolutionary dynamics. *Proceedings of the National Academy of Sciences of the United States of America*, 109: 722–727.
- FLORES, J.-A., JOHNSON, J. E., MEJÍA-MOLINA, A. E., ALVAREZ, M. C., SIERRO, F. J., SINGH, S. D., MAHANTI, S. and GIOSAN, L., 2014. Sedimentation rates from calcareous nannofossil and planktonic foraminifera biostratigraphy in the Andaman Sea, northern Bay of Bengal, and Eastern Arabian Sea. *Marine and Petroleum Geology*, 58: 425–437.
- FLOWER, B. P. and KENNEDY, J. P., 1994. Middle Miocene deepwater paleoceanography in the southwest Pacific: relations with East Antarctic ice sheet development. *Paleoceanography*, 10: 1095–1112.
- GBIF.ORG 2021. GBIF Home Page. www.gbif.org (accessed on 4/1/2021).
- GREEN, O. R., 2001. Extraction Techniques for Acid Insoluble Microfossils. In: Green, O.R., Eds., *A Manual of Practical Laboratory and Field Techniques in Palaeobiology*, 290–291, Netherlands: Springer.
- HERNÁNDEZ-ALMEIDA, I., BOLTOVSKOY, D., KRUGLIKOVÁ, S. B. and CORTESE, G., 2020. Radiolarian census counts and radiolarian-based temperature reconstructions from sediment cores in the Pacific Ocean. *Pangaea*. doi: 10.1594/PANGAEA.923059
- HOLBOURN, A., KUHNT, W., KOCHHANN, K. G. D., ANDERSEN, N. and MEIER, K. J. S., 2015. Global perturbation of the carbon cycle at the onset of the Miocene Climatic Optimum. *Geology*, 43: 123–126.
- JACOT DES COMBES, H. and ABELMANN, A., 2007. A 350-ky radiolarian record off Lüderitz, Namibia - evidence for changes in the upwelling regime. *Marine Micropaleontology*, 62 (3): 194–210.
- JOHNSON, D. A., 1974. Radiolaria from the eastern Indian Ocean, DSDP Leg 22. *Initial Reports of the Deep Sea Drilling Project*, 22: 521–575.
- , 1990. Radiolarian biostratigraphy in the Central Indian Ocean, Leg 115. *Proceedings of the Ocean Drilling Program. Scientific Results*, 115, 395–409.
- JOHNSON, D. A. and NIGRINI, C. A., 1985. Synchronous and time-transgressive Neogene radiolarian datum levels in the equatorial Indian and Pacific Oceans. *Marine Micropaleontology*, 9 (6): 489–523.
- JØRGENSEN, E., 1905. The Protist plankton and the diatoms in bottom samples. VII. Radiolaria. In: Nordgaard O., Ed, *Hydrographical and Biological Investigations in Norwegian Fiords*, 114–142. Norway: Bergens Museum.
- KAMIKURI, S. I., MOTOYAMA, I., NISHI, H. and IWAI, M., 2009a. Neogene radiolarian biostratigraphy and faunal evolution rates in the eastern equatorial Pacific ODP Sites 845 and 1241. *Acta Palaeontologica Polonica*, 54 (4): 713–742.
- , 2009b. Evolution of Eastern Pacific Warm Pool and upwelling processes since the middle Miocene based on analysis of radiolarian assemblages: Response to Indonesian and Central American Seaways. *Palaeogeography, Palaeoclimatology, Palaeoecology*, 280 (3–4): 469–479.
- KAMIKURI, S. I., ITAKI, T., MOTOYAMA, I. and MATSUZAKI, K. M., 2017. Radiolarian biostratigraphy from middle Miocene to late Pleistocene in the Japan Sea. *Paleontological Research*, 21 (4): 397–421.
- LABRACHERIE, M., DE GRACIANSKY, P. C. and POAG, C. W., 2005. Radiolaria abundance of Hole 80–548. *Pangaea*. doi: 10.1594/PANGAEA.250351
- LAZARUS, D., 2005. A brief review of radiolarian research. *Paläontologische Zeitschrift*, 79: 183–200. doi: 10.1007/BF03021761.
- LAZARUS, D., BITTNIOK, B., DIESTER-HAASS, L., MEYERS, P. and BILLUPS, K., 2006. Comparison of radiolarian and sedimentologic paleoproductivity proxies in the latest Miocene-Recent Benguela Upwelling System. *Marine Micropaleontology*, 60: 269–294.
- LAZARUS, D., FAUST, K. and POPOVA-GOLL, I., 2005. New species of prunoid radiolarians from the Antarctic Neogene. *Journal of Micropalaeontology*, 24 (2): 97–121.
- LAZARUS, D., SPENCER-CERVATO, C., PIKA-BIOLZI, M., BECKMANN, J.P., VON SALIS, K., HILBRECHT, H. and THIERSTEIN, H.R., 1995. Revised chronology of Neogene DSDP holes from the world ocean, Technical note 24, 312. College Station, TX: Ocean Drilling Program, doi: 10.2973/odp.tn.24.1995
- LEVYKINA, L. E. 1986. Stratigraphy of Neogene deposits in North-West Pacific according to radiolarians. *Transactions of the Geological Institute, USSR Academy of Sciences*, 413: 116.
- LI, C.-F., LIN, J., KULHANEK, D.K., WILLIAMS, T., BAO, R., BRIAIS, A., BROWN, E.A., CHEN, Y., CLIFT, P.D., COLWELL,

- F.S., DADD, K.A., DING, W., HERNÁNDEZ ALMEIDA, I., HUANG, X.-L., HYUN, S., JIANG, T., KOPPERS, A.A.P., LI, Q., LIU, C., LIU, Q., LIU, Z., NAGAI, R.H., PELEO-ALAMPAY, A., SU, X., SUN, Z., TEJADA, M.L.G., TRINH, H.S., YEH, Y.-C., ZHANG, C., ZHANG, F., ZHANG, G.-L. and ZHAO, X., 2015. Methods. In: Li, C.-F., Lin, J., Kulhanek, D.K. and the Expedition 349 Scientists, Eds., *Proceedings of the Integrated Ocean Discovery Program, 349: South China Sea Tectonics*, 1–56, TX: College Station. doi: 10.14379/iodp.proc.349.102.2015
- LING, H. Y., LUYENDYK, B. P. and CANN, J. R., 2005. Radiolaria abundance of Hole 49–407. *Pangaea*. doi.org/10.1594/PANGAEA.250422
- MAHAPATRA, A. and SHARMA, V., 1994. Trissocyctid Radiolaria from the Late Early Miocene Sequences of Colebrook, North Passage and Great Nicobar Islands, Northeast Indian Ocean. *Micropaleontology*, 40 (2): 157–168.
- MATHUR, K., 1973. Studies in the fossil microflora of Andaman Islands-2: fossil diatoms from Havelock Island. *Geophytology*, 3: 103–134.
- MCINERNEY, F. and WING, S. L., 2011. The Paleocene-Eocene Thermal Maximum: a perturbation of carbon cycle, climate, and biosphere with implications for the future. *Annual Review of Earth and Planetary Sciences*, 39: 489–516.
- MODESTOU, S. E., LEUTERT, T. J., FERNANDEZ, A., LEAR, C. H. and MECKLER, A. N., 2020. Warm middle Miocene Indian Ocean bottom water temperatures: Comparison of clumped isotope and Mg/Ca-based estimates. *Paleoceanography and Paleoclimatology*, 35 (11): e2020PA003927 doi: 10.1029/2020PA003927
- NIGRINI, C. and SANFILIPPO, A., 2001. Cenozoic radiolarian stratigraphy for low and middle latitudes, Technical Note 27. College Station TX: Ocean Drilling Program. 1–486 pp. doi:10.2973/odp.tn.27.2001
- NIMMERGUT, A. and ABELMANN, A., 2002. Spatial and seasonal changes of radiolarian standing stocks in the Sea of Okhotsk. Deep Sea Research Part I: *Oceanographic Research Papers*, 49: 463–493.
- ORIGIN PRO 8.0, VERSION, 2007. OriginLab Corporation, USA: Northampton, MA.
- PANGAEA. Data Publisher for Earth and Environmental Science. www.pangaea.de (accessed on 30/4/2021)
- PANT, S. C. and BANDOPADHAYA, S., 1972. Calcareous nanoplankton from Ritchie's Archipelago, Andaman. *Indian Minerals*, 26 (2): 73–76.
- RAI, A. K. and MAURYA, A. S., 2009. Effect of Miocene paleoceanographic changes on the benthic foraminiferal diversity at ODP Site 754A (southeastern Indian Ocean). *Indian Journal of Marine Sciences*, 38: 423–431.
- RAJSHEKHAR, C. and REDDY, P. P., 2003. Quaternary stratigraphy of Andaman-Nicobar Islands, Bay of Bengal. *Journal of the Geological Society of India*, 62: 485–493.
- RAMSAY, A. T. S., SMART, C. W. and ZACHOS, J. C. 1998. A model of early to middle Miocene deep ocean circulation for the Atlantic and Indian oceans. In: A. Cramp et al., Eds., *Geological evolution of Ocean Basins: Results from the Ocean Drilling Program*, 55–70, London: Geological Society of London.
- RIEDEL, W. R. and SANFILIPPO, A. 1970. Radiolaria, Leg 4, Deep Sea Drilling Project. *Initial Reports of the Deep Sea Drilling Project*, 4: 503–575,
- , 1971. Cenozoic Radiolaria from the western tropical Pacific, Leg 7. *Initial Reports of the Deep Sea Drilling Project*, 1529–1672.
- , 1978. Stratigraphy and evolution of tropical Cenozoic radiolarians. *Micropaleontology*, 24 (1): 61–96.
- SANFILIPPO, A. and NIGRINI, C., 1995. Radiolarian stratigraphy across the Oligocene/Miocene transition. *Marine Micropaleontology*, 24 (3–4): 239–285.
- , 1998. Code numbers for Cenozoic lowlatitude radiolarian biostratigraphic zones and GPTS conversion tables. *Marine Micropaleontology*, 33 (1–2): 109–156.
- SANFILIPPO, A. and RIEDEL, W. R., 1974. Radiolaria from the West-Central Indian Ocean and Gulf of Aden, DSDP Leg 24. *Initial Reports of the Deep Sea Drilling Project*, 24: 997–1035.
- SAXENA, S., CHAKRABORTY, A., GHOSH, A. K., DEY, R., ROY, L. and KESHRI, J. P., 2021. Burdigalian to Early Serravallian Diatom Biostratigraphy from Havelock Island, Northern Indian Ocean. *Stratigraphy and Geological Correlation*, 29 (2): 241–262.
- SCHRÖDER-RITZRAU, A., 2001. Radiolaria assemblage in sediment core GIK23414-6. *Pangaea*. doi: 10.1594/PANGAEA.60264
- SHARMA, V. and DANESIAN, J., 1998. Miocene Radiolaria from Nicholson and John Lawrence Islands, Andaman Sea. *Journal of Geological Society of India*, 52 (6): 695–707.
- , 2003. Early Neogene radiolarian changes in the Northeast Indian Ocean and paleoceanographic implications: Evidence from the Andaman-Nicobar Islands. *Proc. 8th International Congress on Pacific Neogene Stratigraphy*, 126–158, Chiang Mai, Thailand.
- SHARMA, V. and RAM, M. P., 2003. Early to middle Miocene radiolarian assemblages and biostratigraphy, Andaman Islands, northeast Indian Ocean. *Journal of the Paleontological Society of India*, 48: 1–39.
- SHARMA, V. and SRINIVASAN, M. S., 2007. *Geology of Andaman-Nicobar: The Neogene Biostratigraphy of Neill Island, Andaman Sea*. New Delhi: Capital Publishing Company, 1–164 pp.
- SHARMA, V., DANESIAN, J., and DEVI, L.B., 2007. Miocene Radiolaria from Inglis Island, Andaman Sea. *Journal of Geological Society of India*, 70 (6): 939–949.
- , 2011. Early Neogene Radiolarian Faunal Turnover in the Northeast Indian Ocean: Evidence from Andaman-Nicobar. *Journal of the Geological Society of India*, 78 (2): 157.
- SHARMA, V., SINGH, S. and RAWAL, N., 1999. Early Middle Miocene Radiolaria from Nicobar Islands, Northeast Indian Ocean. *Micropaleontology*, 45 (3): 251–277.
- SHARMA, V. and DEVI, L. B., 2007. New radiolarian zones in the Early to Middle Miocene of Andaman-Nicobar, Northern Indian Ocean. *Journal of the Palaeontological Society of India*, 52: 155–158.
- SINGH, O. P., 2007. Early Neogene calcareous nannofossils from Lacam Point Section, Havelock Island, Ritchie's Archipelago, Andaman Sea. *Journal of the Geological Society of India*, 60: 363–370.
- SINGH, S.C. and MOEREMANS, R., 2017. *Anatomy of the Andaman-Nicobar subduction system from seismic reflection data*, London: Geological Society, Memoirs 47 (1): 193–204 pp.
- SRINIVASAN, M. S., 1978. New Chronostratigraphic divisions of the Andaman-Nicobar Late Cenozoic. *Recent Researches in Geology*, vol. 4: 22–36. New Delhi: Hindustan Publishing Corporation.

- , 1986. Geology of Andaman-Nicobar Islands. *Journal of Andaman Science Association*, Port Blair, 2 (1): 1–12.
- SRINIVASAN, M. S. and AZMI, R. J., 1976. Paleobathymetric trends of the Late Cenozoic foraminiferal assemblages of Ritchie's Archipelago, Andaman Sea. In: Srinivasan, M. S. Ed., *Proceedings of the VI Indian Colloquium on Micropaleontology and Stratigraphy*, 328–354, Varanasi: BHU.
- SUZUKI, N., 2009. Radiolarian studies by Christian Gottfried Ehrenberg (1795–1876) and value of his species as type species of genera. In: Tanimura, Y. and Aita, Y., Eds., *Reexamination of the Haeckel and Ehrenberg Microfossil Collections as a Historical and Scientific Legacy*, Monograph No. 40. 55–70, Tokyo: Japan National Museum of Nature and Science.
- TAKAHASHI, K., 1990. Radiolarians from the distal Bengal Fan in the equatorial Indian Ocean. *Proceedings of the Ocean Drilling Program, Scientific Results*, 116: 207–212.
- WELLING, L., 2003. Counts of polycystine radiolarian at station TT011\_1-MOC56. *Pangaea*. doi: 10.1594/PANGAEA.123380
- ZHANG, Q., CHEN, M., ZHANG, L., WANG, R., XIANG, R. and HU, W., 2014. Radiolarian biostratigraphy in the southern Bering Sea since Pliocene. *Science China Earth Sciences*, 57 (4): 682–692.